Continuum Mech. Thermodyn.
https://doi.org/10.1007/s00161-019-00758-2

ORIGINAL ARTICLE

Vitaly A. Kuzkin

Thermal equilibration in infinite harmonic crystals

Received: 26 September 2018 / Accepted: 4 March 2019

Abstract We study transient thermal processes in infinite harmonic crystals having a unit cell with an arbitrary number of particles. Initially, particles have zero displacements and random velocities such that spatial distribution of temperature is uniform. Initial kinetic and potential energies are different and therefore the system is far from thermal equilibrium. Time evolution of kinetic temperatures, corresponding to different degrees of freedom of the unit cell, is investigated. It is shown that the temperatures oscillate in time and tend to generally different equilibrium values. The oscillations are caused by two physical processes: equilibration of kinetic and potential energies and redistribution of temperature among degrees of freedom of the unit cell. An exact formula describing these oscillations is obtained. At large times, a crystal approaches thermal equilibrium, i.e., a state in which the temperatures are constant in time. A relation, referred to as the non-equipartition theorem, between equilibrium values of the temperatures and initial conditions is derived. For illustration, transient thermal processes in a diatomic chain and graphene lattice are considered. Analytical results are supported by numerical solution of lattice dynamics equations.

Keywords Thermal equilibrium · Stationary state · Approach to equilibrium · Polyatomic crystal · Complex lattice · Kinetic temperature · Harmonic crystal · Transient processes · Equipartition theorem · Non-equipartition theorem · Temperature matrix

1 Introduction

In classical systems at thermal equilibrium, the kinetic energy of thermal motion of atoms is usually equally shared among degrees of freedom. This fact follows from the equipartition theorem [25,66]. The theorem allows to characterize thermal state of the system by a single scalar parameter, notably the kinetic temperature, proportional to kinetic energy of thermal motion.

Far from thermal equilibrium, kinetic energies, corresponding to different degrees of freedom, can be different [8,16,23,24,26,48]. Therefore, in many works several temperatures are introduced [8,16,29,30,48]. For example, it is well known that temperatures of a lattice and electrons in solids under laser excitation are different (see, e.g., a review paper [48]). Two temperatures are also observed in molecular dynamics simulations of shock waves. In papers [23,24,26,64], it is shown that kinetic temperatures, corresponding to thermal motion of atoms along and across the shock wave front, are different. Different nonequilibrium

Communicated by Andreas Öchsner.

V. A. Kuzkin (✉)
Institute for Problems in Mechanical Engineering RAS (IPME), Saint Petersburg, Russia
E-mail: kuzkinva@gmail.com

V. A. Kuzkin
Peter the Great Saint Petersburg Polytechnical University (SPbPU), Saint Petersburg, Russia

Published online: 12 March 2019

temperatures of sublattices of methylammonium lead halide are reported in papers [10,16]. In papers [31,32], stationary heat transfer in a harmonic diatomic chain connecting two thermal reservoirs is considered. It is shown that temperatures of sublattices at the nonequilibrium steady state are different. Similar phenomenon is observed in the case of unsteady heat transport [45]. In paper [45], it is shown that temperatures of sublattices in heat conducting diatomic chain are different even if their initial values are equal.

In the absence of external excitations, the nonequilibrium system tends to thermal equilibrium. Approach to thermal equilibrium is accompanied by several physical processes. Distribution of velocities tends to Gaussian [13,22,34,46,61]. The total energy is redistributed among kinetic and potential forms [1,2,34,37,43,59]. Kinetic energy is redistributed between degrees of freedom [43]. The energy is redistributed between normal modes [55]. These processes, except for the last one, are present in both harmonic and anharmonic systems [1,13,34,37,43,46,61]. In harmonic crystals, energies of normal modes do not equilibrate. However, distribution of kinetic temperature in infinite harmonic crystals tends to become spatially and temporary uniform [22,44,61]. Therefore, the notion of thermal equilibrium is widely applied to infinite harmonic crystals [7,12–14,21,28,46,61,63].

Approach to thermal equilibrium in harmonic crystals is studied in many works [7,12–14,21,22,28,34, 37,42–44,46,47,52,61]. Various aspects of this process are studied, including existence of the equilibrium state [46], ergodicity [21,63], convergence of the velocity distribution function [7,13,14,34], evolution of entropy [27,28,60], etc. In the present paper, we focus on behavior of the main observable, notably kinetic temperature (temperatures).

Two different approaches for analytical treatment of harmonic crystals are presented in the literature. One approach employs an exact solution of equations of motion [17,22,28,34,47]. Given known the exact solution, kinetic temperature is calculated as mathematical expectation of corresponding kinetic energy. For example, in pioneering work of Klein and Prigogine [34], transition to thermal equilibrium in an infinite harmonic one-dimensional chain with random initial conditions is investigated. Using exact solution derived by Schrödinger [58], it is shown that kinetic and potential energies of the chain oscillate in time and tend to equal equilibrium values [34]. Another approach uses covariances[1] of particle velocities and covariances of displacements as main variables. For harmonic crystals, closed system of equations for covariances can be derived in steady [31,49,56] and unsteady cases [18,37,42–44,50]. Solution of these equations describes, in particular, time evolution of kinetic temperature. In papers [37,42–44], this idea is employed for description of approach to thermal equilibrium in harmonic crystals with *simple* (monoatomic) lattice.[2] In particular, monoatomic one-dimensional chains [2,37] and two-dimensional lattices [42–44] are considered. However, closed-form expressions describing time evolution of kinetic temperature during thermal equilibration have been derived only for several particular lattices. Below, we derive a general expression for kinetic temperature valid for a wide class of lattices.

In the present paper, we study an approach toward thermal equilibrium in infinite harmonic crystals having a unit cell with an arbitrary number of particles (sometimes such crystals are refereed to as *polyatomic* [41]). Our main goals are to describe time evolution of kinetic temperatures, corresponding to different degrees of freedom of the unit cell, and to calculate equilibrium values of these temperatures.

The paper is organized as follows. In Sect. 2, equations of motion for the unit cell are represented in a matrix form. It allows to cover monoatomic and polyatomic lattices with interaction of an arbitrary number of neighbors and harmonic on-site potential. In Sect. 3, approach to thermal equilibrium is considered. An equation describing time evolution of kinetic temperatures, corresponding to different degrees of freedom of the unit cell, is derived. An exact solution of this equation is obtained. In Sect. 4, an expression relating equilibrium values of the temperatures with initial conditions is derived. In Sects. 5 and 6, approach to thermal equilibrium in a diatomic chain and graphene lattice are studied. Obtained results are exact in the case of spatially uniform distribution of temperature in infinite harmonic crystals. Implications of the nonuniform temperature distribution and anharmonic effects are discussed in Sect. 7.

2 Equations of motion and initial conditions

We consider infinite crystals with unit cell containing an arbitrary number of particles in d-dimensional space ($d = 1, 2, 3$). In this section, equations of motion of the unit cell are written in a matrix form, convenient for analytical derivations.

[1] Covariance of two centered random values is equal to mathematical expectation of their product.

[2] A lattice is referred to as simple lattice, if it coincides with itself under shift by a vector connecting any two particles.

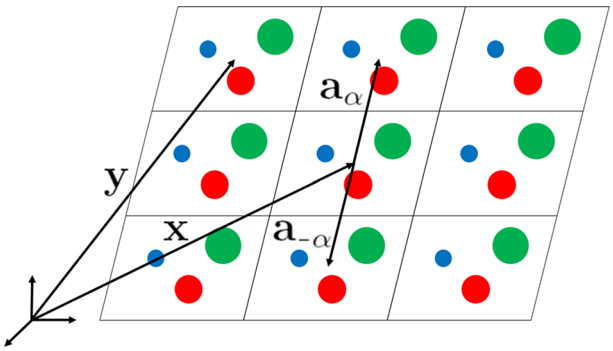

Fig. 1 A two-dimensional polyatomic crystal with three sublattices. Particles forming sublattices have different colors and sizes

Elementary cells of the lattice are identified by their position vectors, $\mathbf{x}$, in the undeformed state.[3] Each elementary cell has N degrees of freedom $u_i(\mathbf{x}), i = 1, \ldots, N$, corresponding to components of particles displacements. The components of displacements form a column:

$$\boldsymbol{u}(\mathbf{x}) = \left[u_1\ u_2\ \cdots\ u_N\right]^\top, \tag{1}$$

where $\top$ stands for the transpose sign.

Remark Here and below, matrices are denoted by bold italic symbols, while invariant vectors, e.g., position vector, are denoted by bold symbols.

Particles from the cell $\mathbf{x}$ interact with each other and with particles from neighboring unit cells, numbered by index α. Vector connecting the cell $\mathbf{x}$ with neighboring cell number α is denoted $\mathbf{a}_\alpha$. Centers of unit cells always form a simple lattice, therefore numbering can be carried out so that vectors $\mathbf{a}_\alpha$ satisfy the identity:

$$\mathbf{a}_\alpha = -\mathbf{a}_{-\alpha}. \tag{2}$$

Here, $\mathbf{a}_0 = 0$. Vectors $\mathbf{a}_\alpha$ for a sample lattice are shown in Fig. 1.

In the present paper, an infinite crystal is considered as a limiting case of a crystal under periodic boundary conditions. The periodic cell contains n^d unit cells (n in each direction). Displacements of particles satisfy periodic boundary conditions:

$$\boldsymbol{u}(\mathbf{x}) = \boldsymbol{u}\left(\mathbf{x} + \sum_{j=1}^{d} C_j n \mathbf{b}_j\right), \tag{3}$$

where $\mathbf{b}_j$ are primitive vectors of the lattice; C_j are integers. Further, analytical derivations are carried out for $n \to \infty$, while in computer simulations n is finite.

Consider equations of motion of the unit cell. In harmonic crystals, the total force acting on each particle is represented as a linear combination of displacements of all other particles. Using this fact, we write equations of motion in the form:[4]

$$\boldsymbol{M}\dot{\boldsymbol{v}}(\mathbf{x}) = \sum_\alpha \boldsymbol{C}_\alpha \boldsymbol{u}(\mathbf{x} + \mathbf{a}_\alpha), \qquad \boldsymbol{C}_\alpha = \boldsymbol{C}_{-\alpha}^\top, \tag{4}$$

where $\boldsymbol{v} = \dot{\boldsymbol{u}}$; $\boldsymbol{u}(\mathbf{x}+\mathbf{a}_\alpha)$ is a column of displacements of particles from unit cell α; $\boldsymbol{M}$ is diagonal $N \times N$ matrix composed of particles' masses; for $\alpha \neq 0$ coefficients of $N \times N$ matrix $\boldsymbol{C}_\alpha$ determine stiffness of springs connecting unit cell $\mathbf{x}$ with neighboring cell number α; matrix $\boldsymbol{C}_0$ describes interactions of particles inside[5] the unit cell $\mathbf{x}$. Summation is carried out with respect to all unit cells α, interacting with unit cell $\mathbf{x}$ (including $\alpha = 0$).

Remark Equations of motion (4) are valid for crystals with interactions of an arbitrary number of neighbors.

Remark Relation $\boldsymbol{C}_\alpha = \boldsymbol{C}_{-\alpha}^\top$ in formula (4) guarantees that dynamical matrix of the lattice is Hermitian (see Sect. 3.2 and "Appendix II").

[3] For analytical derivations, position vectors are more convenient than indices, because number of indices depends on space dimensionality.

[4] Similar form of equations of motion is used in paper [52].

[5] Additionally, matrix $\boldsymbol{C}_0$ can include stiffness of harmonic on-site potential.

Formula (4) describes motion of monoatomic and polyatomic crystals in one-, two-, and three-dimensional cases. For $N = 1$ (one degree of freedom per unit cell), Eq. (4) governs dynamics of the so-called scalar lattices,[6] considered, for example, in papers [19,44,52,53]. Below, we consider two particular polyatomic crystals, notably one-dimensional diatomic chain and two-dimensional graphene sheet (see Sects. 5 and 6). Matrices $\boldsymbol{M}$, $\boldsymbol{C}_\alpha$ for these lattices are given by formulas (38) and (50).

The following initial conditions, typical for molecular dynamics modeling [1], are considered:

$$\boldsymbol{u}(\mathbf{x}) = 0, \quad \boldsymbol{v}(\mathbf{x}) = \boldsymbol{v}_0(\mathbf{x}). \tag{5}$$

Here, $\boldsymbol{v}_0(\mathbf{x})$ is a column of random initial velocities of particles from unit cell $\mathbf{x}$ such that

$$\left\langle \boldsymbol{v}_0(\mathbf{x}) \right\rangle = 0, \qquad \left\langle \boldsymbol{v}_0(\mathbf{x}) \boldsymbol{v}_0(\mathbf{y}) \right\rangle = \boldsymbol{A}\delta_D(\mathbf{x}-\mathbf{y}), \tag{6}$$

where $\left\langle \cdots \right\rangle$ stands for mathematical expectation;[7] $\delta_D(0) = 1$; $\delta_D(\mathbf{x}-\mathbf{y}) = 0$ for $\mathbf{x} \neq \mathbf{y}$; $\boldsymbol{A}$ is a constant matrix independent of $\mathbf{x}$ and $\mathbf{y}$. In other words, components of $\boldsymbol{v}_0(\mathbf{x})$ are random numbers with zero mean[8] and generally different variances given by diagonal elements of matrix $\boldsymbol{A}$. Off-diagonal elements of matrix $\boldsymbol{A}$ are equal to covariances of initial velocities, corresponding to different degrees of freedom of the unit cell. Initial velocities of particles from different unit cells are statistically independent. Examples of initial conditions (5) are given by formulas (39) and (51).

From macroscopic point of view, initial conditions (5), (6) correspond to *uniform* spatial distribution of temperature.

Equations of motion (4) with initial conditions (5) completely determine dynamics of a crystal at any moment in time. The equations can be solved analytically using, for example, discrete Fourier transform. Resulting random velocities of the particles can be used for calculation of statistical characteristics, such as kinetic temperature. However in the following sections, we use another approach [37], which allows to formulate and solve equations for statistical characteristics of the crystal with *deterministic* initial conditions.

3 Thermal equilibration

Initial conditions (5) are such that initially kinetic and potential energies of the crystal are different (potential energy is equal to zero). Motion of particles leads to redistribution of energy among kinetic and potential forms. Therefore kinetic temperature, proportional to kinetic energy, changes in time. In this section, we derive a formula, exactly describing time evolution of kinetic temperatures, corresponding to different degrees of freedom of the unit cell. The formula shows that a crystal evolves toward a state in which the temperatures are constant in time. This state is further refereed to as the *thermal equilibrium*.

3.1 Kinetic temperature and temperature matrix

In this section, we derive an equation, exactly describing time evolution of the kinetic temperatures during approach to thermal equilibrium.

We consider an infinite set of realizations of the same system. The realizations differ only by random initial conditions (5). This approach allows to introduce statistical characteristics such as kinetic temperatures.

In general, each degree of freedom of the unit cell has its own kinetic energy and kinetic temperature. Then in order to characterize thermal state of the unit cell, we introduce $N \times N$ matrix, $\boldsymbol{T}$, further referred to as the *temperature matrix*:

$$k_\mathrm{B}\boldsymbol{T}(\mathbf{x}) = \boldsymbol{M}^{\frac{1}{2}}\left\langle \boldsymbol{v}(\mathbf{x})\boldsymbol{v}(\mathbf{x})^\top \right\rangle \boldsymbol{M}^{\frac{1}{2}} \quad \Leftrightarrow \quad k_\mathrm{B}T_{ij} = \sqrt{M_i M_j}\left\langle v_i v_j \right\rangle, \tag{7}$$

[6] In scalar lattices, each particle has only one degree of freedom. This model is applicable to monoatomic one-dimensional chains with interactions of arbitrary number of neighbors and to out-of-plane motions of monoatomic two-dimensional lattices.

[7] In computer simulations, mathematical expectation is approximated by average over realizations with different random initial conditions.

[8] In this case, mathematical expectations of all velocities are equal to zero at any moment in time.

where $\boldsymbol{M}^{\frac{1}{2}}\boldsymbol{M}^{\frac{1}{2}} = \boldsymbol{M}$; M_i is ith element of matrix $\boldsymbol{M}$, equal to a mass corresponding to ith degree of freedom of the unit cell; k_B is the Boltzmann constant. Diagonal element, T_{ii}, of the temperature matrix is equal to kinetic temperature, corresponding to ith degrees of freedom of the unit cell, i.e., $k_\mathrm{B}T_{ii} = M_i\left\langle v_i^2\right\rangle$. Off-diagonal elements characterize correlation between components of velocities, corresponding to different degrees of freedom.

We also introduce the kinetic temperature, T, proportional to the total kinetic energy of the unit cell:

$$T = \frac{1}{N}\operatorname{tr}\boldsymbol{T} = \frac{1}{N}\sum_{i=1}^{N} T_{ii}, \tag{8}$$

where N is a number of degrees of freedom per unit cell; $\operatorname{tr}(\cdots)$ stands for trace[9] of a matrix. In the case of energy equipartition, kinetic temperatures, corresponding to all degrees of freedom of the unit cell, are equal to T.

Neither kinetic temperature (8) nor temperature matrix (7) is sufficient for derivation of closed system of equations [37]. Therefore, we introduce generalized kinetic energy $\boldsymbol{K}(\mathbf{x},\mathbf{y})$ defined for any pair of unit cells $\mathbf{x}$ and $\mathbf{y}$ as

$$\boldsymbol{K}(\mathbf{x},\mathbf{y}) = \frac{1}{2}\boldsymbol{M}^{\frac{1}{2}}\left\langle \boldsymbol{v}(\mathbf{x})\boldsymbol{v}(\mathbf{y})^{\top}\right\rangle\boldsymbol{M}^{\frac{1}{2}}. \tag{9}$$

Diagonal elements of matrix $\boldsymbol{K}(\mathbf{x},\mathbf{x})$ are equal to mathematical expectations of kinetic energies, corresponding to different degrees of freedom of the unit cell, i.e., $K_{ii}(\mathbf{x},\mathbf{x}) = \frac{1}{2}M_i\left\langle v_i(\mathbf{x})^2\right\rangle$. The generalized kinetic energy is related to the temperature matrix (7) as

$$\frac{1}{2}k_\mathrm{B}\boldsymbol{T} = \boldsymbol{K}(\mathbf{x},\mathbf{x}). \tag{10}$$

Remark Notion of generalized kinetic energy for monoatomic lattices is introduced in papers [37,42–44]. Note that in papers [37,42–44], the generalized kinetic energy is defined for a pair of particles, while in the present paper it is defined for a pair of unit cells.

Initial conditions (5), (6) are such that spatial distribution of all statistical characteristics is *uniform*. In this case, the following identity is satisfied:

$$\boldsymbol{K}(\mathbf{x},\mathbf{y}) = \boldsymbol{K}(\mathbf{x}-\mathbf{y}). \tag{11}$$

Argument $\mathbf{x}-\mathbf{y}$ is omitted below for brevity. In "Appendix I," it is shown that the generalized kinetic energy, $\boldsymbol{K}(\mathbf{x}-\mathbf{y})$, satisfies equation:

$$\begin{aligned} &\dddot{\boldsymbol{K}} - 2\left(\boldsymbol{\mathcal{L}}\ddot{\boldsymbol{K}} + \ddot{\boldsymbol{K}}\boldsymbol{\mathcal{L}}\right) + \boldsymbol{\mathcal{L}}^2\boldsymbol{K} - 2\boldsymbol{\mathcal{L}}\boldsymbol{K}\boldsymbol{\mathcal{L}} + \boldsymbol{K}\boldsymbol{\mathcal{L}}^2 = 0,\\ &\boldsymbol{\mathcal{L}}\boldsymbol{K} \stackrel{\text{def}}{=} \sum_{\alpha}\boldsymbol{M}^{-\frac{1}{2}}\boldsymbol{C}_\alpha\boldsymbol{M}^{-\frac{1}{2}}\boldsymbol{K}(\mathbf{x}-\mathbf{y}+\mathbf{a}_\alpha). \end{aligned} \tag{12}$$

Here, $\boldsymbol{\mathcal{L}}^2\boldsymbol{K} = \boldsymbol{\mathcal{L}}(\boldsymbol{\mathcal{L}}\boldsymbol{K})$. Formula (12) is equivalent to an infinite system of ordinary differential equations. It *exactly* describes the evolution of generalized kinetic energy in any harmonic lattice.

Remark A particular case of Eq. (12) for a one-dimensional monoatomic harmonic chain with nearest-neighbor interactions was originally derived in papers [36,37].

Remark Consider physical meaning of difference operator $\boldsymbol{\mathcal{L}}$. Using this operator, equation of motion (4) is represented as

$$\boldsymbol{M}^{\frac{1}{2}}\ddot{\boldsymbol{u}}(\mathbf{x}) = \boldsymbol{M}^{-\frac{1}{2}}\sum_{\alpha}\boldsymbol{C}_\alpha\boldsymbol{u}(\mathbf{x}+\mathbf{a}_\alpha) = \boldsymbol{\mathcal{L}}\left(\boldsymbol{M}^{\frac{1}{2}}\boldsymbol{u}(\mathbf{x})\right). \tag{13}$$

Therefore $\boldsymbol{\mathcal{L}}$ is equal to operator in the right-hand side of equations of motion provided that the equations are written for $\boldsymbol{M}^{\frac{1}{2}}\boldsymbol{u}(\mathbf{x})$.

Remark Note that Eq. (12) can be generalized for the case of arbitrary initial conditions, corresponding to nonuniform initial temperature profile (see formula (59)). The generalized equation can be used, e.g., for description of ballistic heat transport. For scalar lattices, this approach is used in papers [18,38,39,44].

[9] Trace of a square matrix is defined as a sum of diagonal elements.

Initial conditions for $\boldsymbol{K}$, corresponding to initial conditions for particle velocities (5), (6), have the form:

$$\boldsymbol{K} = \boldsymbol{K}_0 = \frac{1}{2} k_\mathrm{B} \boldsymbol{T}_0 \delta_D(\mathbf{x}-\mathbf{y}), \qquad \dot{\boldsymbol{K}} = 0, \qquad \ddot{\boldsymbol{K}} = \boldsymbol{\mathcal{L}}\boldsymbol{K}_0 + \boldsymbol{K}_0\boldsymbol{\mathcal{L}}, \quad \dddot{\boldsymbol{K}} = 0, \tag{14}$$

where $\boldsymbol{T}_0$ is the initial value of temperature matrix (7), independent of $\mathbf{x}$. Here, the expression for $\boldsymbol{K}$ follows from formulas (7), (10) and initial conditions (5), (6). Values $\dot{\boldsymbol{K}}$ and $\dddot{\boldsymbol{K}}$ are proportional to covariance of displacements and velocities. Since initial displacements are equal to zero, then initial values of $\dot{\boldsymbol{K}}$, $\dddot{\boldsymbol{K}}$ vanish. The expression for $\ddot{\boldsymbol{K}}$ follows from formula (58), derived in "Appendix I."

Thus, the generalized kinetic energy $\boldsymbol{K}(\mathbf{x}-\mathbf{y})$ satisfies Eq. (12) with *deterministic* initial conditions (14). Given known the solution of this initial value problem, the temperature matrix, $\boldsymbol{T}$, is calculated using formula (7).

3.2 Time evolution of the temperature matrix

In this section, we solve Eq. (12) for the generalized kinetic energy with initial conditions (14). The solution yields *an exact* expression for the temperature matrix at any moment in time.

The solution is obtained using the discrete Fourier transform with respect to variable $\mathbf{x}-\mathbf{y}$. Vectors $\mathbf{x}-\mathbf{y}$ form the same lattice as vectors $\mathbf{x}$. Then, the vectors are represented as

$$\mathbf{x}-\mathbf{y} = \sum_{j=1}^{d} z_j \mathbf{b}_j, \tag{15}$$

where $\mathbf{b}_j$, $j = 1,\ldots,d$ are primitive vectors of the lattice [35]; z_j are integers; d is space dimensionality. Direct and inverse discrete Fourier transforms for an infinite lattice are defined as

$$\begin{aligned} &\hat{\boldsymbol{K}}(\mathbf{k}) = \sum_{z_1=-\infty}^{+\infty} \ldots \sum_{z_d=-\infty}^{+\infty} \boldsymbol{K}(\mathbf{x}-\mathbf{y}) e^{-\mathrm{i}\mathbf{k}\cdot(\mathbf{x}-\mathbf{y})}, \qquad \mathbf{k} = \sum_{j=1}^{d} p_j \widetilde{\mathbf{b}}_j, \\ &\boldsymbol{K}(\mathbf{x}-\mathbf{y}) = \int_{\mathbf{k}} \hat{\boldsymbol{K}}(\mathbf{k}) e^{\mathrm{i}\mathbf{k}\cdot(\mathbf{x}-\mathbf{y})} \mathrm{d}\mathbf{k}. \end{aligned} \tag{16}$$

Here, $\hat{\boldsymbol{K}}$ is Fourier image of $\boldsymbol{K}$; $\mathrm{i}^2 = -1$; $\mathbf{k}$ is wave vector; $\widetilde{\mathbf{b}}_j$ are vectors of the reciprocal basis, i.e., $\widetilde{\mathbf{b}}_j \cdot \mathbf{b}_k = \delta_{jk}$, where δ_{jk} is the Kronecker delta; for brevity, the following notation is used:

$$\int_{\mathbf{k}} \cdots \mathrm{d}\mathbf{k} = \frac{1}{(2\pi)^d} \int_0^{2\pi} \ldots \int_0^{2\pi} \ldots \mathrm{d}p_1 \ldots \mathrm{d}p_d. \tag{17}$$

Applying the discrete Fourier transform (16) in formulas (12), (14) yields equation[10]

$$\begin{aligned} &\dddot{\hat{\boldsymbol{K}}} + 2\left(\boldsymbol{\Omega}\ddot{\hat{\boldsymbol{K}}} + \ddot{\hat{\boldsymbol{K}}}\boldsymbol{\Omega}\right) + \boldsymbol{\Omega}^2\dot{\hat{\boldsymbol{K}}} - 2\boldsymbol{\Omega}\dot{\hat{\boldsymbol{K}}}\boldsymbol{\Omega} + \dot{\hat{\boldsymbol{K}}}\boldsymbol{\Omega}^2 = 0, \\ &\boldsymbol{\Omega}(\mathbf{k}) = -\sum_{\alpha} \boldsymbol{M}^{-\frac{1}{2}} \boldsymbol{C}_\alpha \boldsymbol{M}^{-\frac{1}{2}} e^{\mathrm{i}\mathbf{k}\cdot\mathbf{a}_\alpha}, \end{aligned} \tag{18}$$

with initial conditions

$$\hat{\boldsymbol{K}} = \frac{1}{2} k_\mathrm{B} \boldsymbol{T}_0, \qquad \dot{\hat{\boldsymbol{K}}} = 0, \qquad \ddot{\hat{\boldsymbol{K}}} = -\frac{1}{2} k_\mathrm{B} \left(\boldsymbol{\Omega}\boldsymbol{T}_0 + \boldsymbol{T}_0\boldsymbol{\Omega}\right), \qquad \dddot{\hat{\boldsymbol{K}}} = 0. \tag{19}$$

Matrix $\boldsymbol{\Omega}$ in formula (18) coincides with the *dynamical matrix* of the lattice, derived in "Appendix II" (see formula (67)). Examples of matrix $\boldsymbol{\Omega}$ for two particular lattices are given by formulas (41), (53).

[10] Here, identities $\Phi\left(\boldsymbol{K}(\mathbf{x}-\mathbf{y}+\mathbf{a}_\alpha)\right) = \hat{\boldsymbol{K}} e^{\mathrm{i}\mathbf{k}\cdot\mathbf{a}_\alpha}$, $\Phi(\delta_D(\mathbf{x}-\mathbf{y})) = 1$, $\Phi\left(\boldsymbol{\mathcal{L}}\boldsymbol{K}\right) = -\boldsymbol{\Omega}\hat{\boldsymbol{K}}$, $\Phi\left(\boldsymbol{\mathcal{L}}^2\boldsymbol{K}\right) = -\boldsymbol{\Omega}\Phi\left(\boldsymbol{\mathcal{L}}\boldsymbol{K}\right) = \boldsymbol{\Omega}^2\hat{\boldsymbol{K}}$ are used. Φ is operator of the discrete Fourier transform, i.e., $\Phi\left(\boldsymbol{K}\right) = \hat{\boldsymbol{K}}$.

To simplify Eq. (18), we use the fact that matrix $\boldsymbol{\Omega}$ is Hermitian, i.e., it is equal to its own conjugate transpose.[11] Then, it can be represented in the form:

$$\boldsymbol{\Omega} = \boldsymbol{P}\boldsymbol{\Lambda}\boldsymbol{P}^{*\top}, \qquad \Lambda_{ij} = \omega_j^2 \delta_{ij}, \tag{20}$$

where ω_j^2, $j = 1, \ldots, N$ are eigenvalues of matrix $\boldsymbol{\Omega}$ and $\omega_j(\mathbf{k})$ are branches of dispersion relation for the lattice (below we consider only nonnegative frequencies, i.e., $\omega_j(\mathbf{k}) \geq 0$); $*$ stands for complex conjugate; matrix[12] $\boldsymbol{P}$ is composed of normalized eigenvectors of matrix $\boldsymbol{\Omega}$. Eigenvectors of the dynamical matrix are referred to as polarization vectors [11]. Examples of matrix $\boldsymbol{P}$ are given by formulas (43) and (55).

We substitute formula (20) into (18) and multiply both parts by $\boldsymbol{P}^{*\top}$ from the left and by $\boldsymbol{P}$ from the right. Then, decoupled system of equations with respect to elements of matrix $\boldsymbol{K}' = \boldsymbol{P}^{*\top}\hat{\boldsymbol{K}}\boldsymbol{P}$ is obtained

$$\begin{aligned} &\dddot{\boldsymbol{K}}' + 2\left(\boldsymbol{\Lambda}\ddot{\boldsymbol{K}}' + \ddot{\boldsymbol{K}}'\boldsymbol{\Lambda}\right) + \boldsymbol{\Lambda}^2\boldsymbol{K}' - 2\boldsymbol{\Lambda}\boldsymbol{K}'\boldsymbol{\Lambda} + \boldsymbol{K}'\boldsymbol{\Lambda}^2 = 0 \\ &\Leftrightarrow \ddddot{K}'_{ij} + 2(\omega_i^2 + \omega_j^2)\ddot{K}'_{ij} + (\omega_i^2 - \omega_j^2)^2 K'_{ij} = 0. \end{aligned} \tag{21}$$

Similar manipulations with formulas (19) give initial conditions for $\boldsymbol{K}'$. Solving Eq. (21) with the initial conditions, using relation (10) for matrices $\boldsymbol{T}$ and $\boldsymbol{K}$, and applying inverse discrete Fourier transform, yields:

$$\boldsymbol{T} = \int_{\mathbf{k}} \boldsymbol{P}\boldsymbol{T}'\boldsymbol{P}^{*\top}\mathrm{d}\mathbf{k}, \qquad T'_{ij} = \frac{1}{2}\{\boldsymbol{P}^{*\top}\boldsymbol{T}_0\boldsymbol{P}\}_{ij}\left[\cos((\omega_i - \omega_j)t) + \cos((\omega_i + \omega_j)t)\right]. \tag{22}$$

Here, $\{\ldots\}_{ij}$ is element i, j of the matrix; $\omega_i(\mathbf{k}) \geq 0$, $i = 1, \ldots, N$. Here and below, integration is carried out with respect to dimensionless components of the wave vector, $\mathbf{k}$ (see formula (17)). Formula (22) is an exact expression for the temperature matrix at any moment in time.

If initial kinetic energy is equally distributed between degrees of freedom of the unit cell, then $\boldsymbol{T}_0 = T_0\boldsymbol{E}$ and formula (22) reduces to

$$\boldsymbol{T} = \frac{T_0}{2}\left(\boldsymbol{E} + \int_{\mathbf{k}} \boldsymbol{P}\boldsymbol{B}(t)\boldsymbol{P}^{*\top}\mathrm{d}\mathbf{k}\right), \qquad B_{ij} = \cos(2\omega_j t)\delta_{ij}, \tag{23}$$

where $\boldsymbol{E}$ is the identity matrix, i.e., $E_{ij} = \delta_{ij}$. Formula (23) shows that during approach to thermal equilibrium, temperature matrix is generally not isotropic,[13] i.e., temperatures, corresponding to degrees of freedom of the unit cell, are generally different even if their initial values are equal.

Remark In general, matrix $\boldsymbol{P}$ is complex-valued (see, e.g., formulas (43), (55)). Therefore, matrices $\boldsymbol{P}^{*\top}\boldsymbol{T}_0\boldsymbol{P}$ and $\boldsymbol{P}\boldsymbol{B}\boldsymbol{P}^{*\top}$ in formulas (22), (23) are also complex-valued. However, resulting temperature matrix is real. This fact can be proven using the following properties $\boldsymbol{P}(\mathbf{k}) = \boldsymbol{P}(-\mathbf{k})^*$, $\omega_j^2(\mathbf{k}) = \omega_j^2(-\mathbf{k})$.

Thus, formula (22) *exactly* describes time evolution of the temperature matrix during approach to thermal equilibrium. The majority of further results follow from formula (22).

3.3 Time evolution of kinetic temperature

In this section, using formula (22) we investigate the evolution of the kinetic temperature, T, defined by formula (8). According to formulas (7), (8), the kinetic temperature is proportional to the total kinetic energy of the unit cell. Since the total energy per unit cell is conserved, the evolution of the kinetic temperature is caused by redistribution of energy among kinetic and potential forms.

Kinetic temperature is calculated using formula (22):[14]

$$T = \frac{T_0}{2}\left[1 + \frac{1}{N}\sum_{j=1}^{N}\int_{\mathbf{k}}\left(1 + \frac{\{\boldsymbol{P}^{*\top}\mathrm{dev}\boldsymbol{T}_0\boldsymbol{P}\}_{jj}}{T_0}\right)\cos\left(2\omega_j(\mathbf{k})t\right)\mathrm{d}\mathbf{k}\right], \tag{24}$$

[11] Proof of this statement is given in "Appendix II."

[12] Matrix $\boldsymbol{P}$ is unitary, i.e., $\boldsymbol{P}\boldsymbol{P}^{*\top} = \boldsymbol{E}$, where $\boldsymbol{E}$ is identity matrix, i.e., $E_{ij} = \delta_{ij}$.

[13] Matrix is called isotropic if it is diagonal and all elements on the diagonal are equal.

[14] Here, the identity $\mathrm{tr}\left(\boldsymbol{P}\boldsymbol{T}'\boldsymbol{P}^{*\top}\right) = \mathrm{tr}\boldsymbol{T}'$ was used.

where $\mathrm{dev}\boldsymbol{T}_0 = \boldsymbol{T}_0 - T_0\boldsymbol{E}$, $T_0 = \frac{1}{N}\mathrm{tr}\boldsymbol{T}_0$, $\boldsymbol{E}$ is identity matrix. Formula (24) shows that evolution of kinetic temperature is influenced by initial distribution of kinetic energy among degrees of freedom of the unit cell. Corresponding example is given in Fig. 5.

If initial kinetic energy is equally distributed among degrees of freedom of the unit cell, then $\mathrm{dev}\boldsymbol{T}_0 = 0$ and formula (24) reduces to

$$T = \frac{T_0}{2}\left[1 + \frac{1}{N}\sum_{j=1}^{N}\int_{\mathbf{k}}\cos\left(2\omega_j(\mathbf{k})t\right)\mathrm{d}\mathbf{k}\right]. \tag{25}$$

This expression can also be derived by calculating trace of both parts in formula (23).

Remark Formula (25) is valid for both monoatomic and polyatomic lattices. It generalizes results obtained in papers [2,37,42,43] for several one-dimensional and two-dimensional monoatomic lattices. For monoatomic scalar lattices ($N = 1$), formula (25) reduces to the expression obtained in paper [44].

Integrands in formulas (24), (25) are rapidly oscillating functions, frequently changing sign inside the integration domain. Integrals of this type usually tend to zero as time tends to infinity [15]. Therefore, kinetic temperature tends to $\frac{T_0}{2}$. Decrease in temperature is caused by redistribution of energy among kinetic and potential forms. Note that this redistribution is *irreversible*.

Remark Calculation of change in entropy corresponding to redistribution of energy between kinetic and potential forms would be an interesting extension of the present work.

Remark Investigation of asymptotic behavior of integrals (24), (25) at large times is not a trivial problem. However, using general results obtained using the stationary phase method [15], we can assume that the value $T - T_0/2$ tends to zero in time as $1/t^{\frac{d}{2}}$, where d is space dimensionality. Confirmation of this assumption for some particular lattices is given in papers [2,37,62]. Rigorous derivation is beyond the scope of the present paper.

Remark Formulas (22), (24), (25) can be generalized for the case of a finite crystal under periodic boundary conditions. In this case, integrals corresponding to inverse discrete Fourier transform are replaced by sums. Effect of finite size of a one-dimensional crystal on approach to thermal equilibrium is studied in paper [54].

Thus, time evolution of the temperature matrix, $\boldsymbol{T}$, during approach to thermal equilibrium, is exactly described by formula (22). The approach is accompanied by two processes: oscillations of kinetic temperature, caused by equilibration of kinetic and potential energies (formulas (24), (25)) and redistribution of kinetic energy between degrees of freedom of the unit cell. From mathematical point of view, the first process is associated with changes in $\mathrm{tr}\boldsymbol{T}$, while the second process causes evolution of $\mathrm{dev}\boldsymbol{T}$.

4 Thermal equilibrium: non-equipartition theorem

4.1 Random initial velocities and zero displacements

In this section, we show that the temperature matrix tends to some equilibrium value constant in time. Therefore, the notion of thermal equilibrium is used. A formula relating equilibrium value of temperature matrix with initial conditions is derived using exact solution (22).

We rewrite formula (22) in the form

$$\begin{aligned}
&\boldsymbol{T} = \frac{1}{2}\int_{\mathbf{k}}\boldsymbol{P}\mathrm{diag}\left(\boldsymbol{P}^{*\top}\boldsymbol{T}_0\boldsymbol{P}\right)\boldsymbol{P}^{*\top}\mathrm{d}\mathbf{k} + \int_{\mathbf{k}}\boldsymbol{P}\widetilde{\boldsymbol{T}}\boldsymbol{P}^{*\top}\mathrm{d}\mathbf{k},\\
&\widetilde{T}_{ij} = \frac{1}{2}\{\boldsymbol{P}^{*\top}\boldsymbol{T}_0\boldsymbol{P}\}_{ij}\left[\cos((\omega_i+\omega_j)t) + \left(1-\delta_{ij}\right)\cos((\omega_i-\omega_j)t)\right].
\end{aligned} \tag{26}$$

Here, diag (. . .) stands for diagonal part of a matrix. The first term in formula (26) is independent of time. In the second term, the integrand is a rapidly oscillating function. Such integrals usually asymptotically tend to zero as $t \to \infty$ (see, e.g., paper [15]). Therefore, the second term vanishes at large times. Then, the temperature matrix tends to equilibrium value, given by the first term. In order to simplify further analysis, we represent matrix $\boldsymbol{T}_0$ as a sum of isotropic part and deviator. Then, the first term in formula (26) reads

$$\boldsymbol{T}_{\mathrm{eq}} = \frac{1}{2N}\mathrm{tr}\left(\boldsymbol{T}_0\right)\boldsymbol{E} + \frac{1}{2}\int_{\mathbf{k}}\boldsymbol{P}\mathrm{diag}\left(\boldsymbol{P}^{*\top}\mathrm{dev}\boldsymbol{T}_0\boldsymbol{P}\right)\boldsymbol{P}^{*\top}\mathrm{d}\mathbf{k}. \tag{27}$$

Formula (27) relates the equilibrium temperature matrix, $\boldsymbol{T}_{\text{eq}}$, with initial conditions. It shows that, in general, equilibrium temperatures, corresponding to different degrees of freedom of the unit cell, are not equal. Formula (27) is a particular case of the *non-equipartition theorem* formulated in the next section.

Formula (27) shows that if initial kinetic temperatures, corresponding to different degrees of freedom of the unit cell, are equal ($\operatorname{dev}\boldsymbol{T}_0 = 0$) then they are also equal at equilibrium ($\operatorname{dev}\boldsymbol{T}_{\text{eq}} = 0$). Note that during approach to equilibrium, the temperature matrix is generally not isotropic, i.e., $\operatorname{dev}\boldsymbol{T} \neq 0$ (see formula (23)).

4.2 Arbitrary initial conditions

In this section, we generalize the results obtained in the previous section for the case of arbitrary initial conditions.

We define generalized potential energy, $\boldsymbol{\Pi}$, generalized Hamiltonian, $\boldsymbol{H}$, and generalized Lagrangian, $\boldsymbol{L}$ as

$$\begin{aligned} &\boldsymbol{H} = \boldsymbol{K} + \boldsymbol{\Pi}, \qquad \boldsymbol{L} = \boldsymbol{K} - \boldsymbol{\Pi}, \qquad \boldsymbol{\Pi} = -\frac{1}{4}\left(\boldsymbol{\mathcal{L}}\boldsymbol{D} + \boldsymbol{D}\boldsymbol{\mathcal{L}}\right), \\ &\boldsymbol{D}(\mathbf{x}-\mathbf{y}) = \boldsymbol{M}^{\frac{1}{2}}\left\langle \boldsymbol{u}(\mathbf{x})\boldsymbol{u}(\mathbf{y})^{\top}\right\rangle \boldsymbol{M}^{\frac{1}{2}}. \end{aligned} \tag{28}$$

In papers [37,43], similar values are introduced for monoatomic lattices.

Consider relation between generalized kinetic and potential energies at thermal equilibrium. In "Appendix I," it is shown that covariance of particle displacements, $\boldsymbol{D}$, and generalized Lagrangian satisfy the identity

$$\boldsymbol{L} = \frac{1}{4}\ddot{\boldsymbol{D}}. \tag{29}$$

We assume that at thermal equilibrium, the second time derivative in the right side of formula (29) is equal to zero. Then, equilibrium values of generalized kinetic and potential energies are equal

$$\boldsymbol{K}_{\text{eq}} = \boldsymbol{\Pi}_{\text{eq}} = \frac{1}{2}\boldsymbol{H}_{\text{eq}}. \tag{30}$$

Consider a system of equations for equilibrium value of the generalized Hamiltonian, $\boldsymbol{H}_{\text{eq}}$. In "Appendix III," it is shown that $\boldsymbol{H}$ satisfies additional conservation laws. Writing the conservation laws for $\boldsymbol{H}_{\text{eq}}$ yields

$$\operatorname{tr}\boldsymbol{H}_{\text{eq}} = \operatorname{tr}\boldsymbol{H}_0, \qquad \operatorname{tr}\left(\boldsymbol{\mathcal{L}}^n \operatorname{dev}\boldsymbol{H}_{\text{eq}}\right) = \operatorname{tr}\left(\boldsymbol{\mathcal{L}}^n \operatorname{dev}\boldsymbol{H}_0\right), \qquad n = 1, 2, \ldots \tag{31}$$

Here, $\boldsymbol{H}_0$ is the initial value of the generalized Hamiltonian. Also $\operatorname{dev}\boldsymbol{H}$ satisfies Eq. (12) (see "Appendix I"). We seek for stationary solution, $\operatorname{dev}\boldsymbol{H}_{\text{eq}}$, of this equation. Then, removing time derivatives in this equation yields:

$$\boldsymbol{\mathcal{L}}^2 \operatorname{dev}\boldsymbol{H}_{\text{eq}} - 2\boldsymbol{\mathcal{L}}\operatorname{dev}\boldsymbol{H}_{\text{eq}}\boldsymbol{\mathcal{L}} + \operatorname{dev}\boldsymbol{H}_{\text{eq}}\boldsymbol{\mathcal{L}}^2 = 0. \tag{32}$$

Solution of Eqs. (31) and (32) yields equilibrium value of the generalized Hamiltonian, $\boldsymbol{H}_{\text{eq}}$. Given known $\boldsymbol{H}_{\text{eq}}$, other generalized energies and temperature matrix are calculated using formulas (10) and (30).

Remark A system of equations, similar to (31), (32), for crystals with monoatomic lattice and interactions of the nearest neighbors was derived in paper [43]. However, solution of this system was obtained only for square and triangular lattices. Here, we derive a general solution of system (31), (32), for any polyatomic lattice.

Equations (31) and (32) are solved as follows. Applying the discrete Fourier transform (16) to these equations, using formula (20) for matrix $\boldsymbol{\Omega}$ and multiplying both parts by $\boldsymbol{P}$ and $\boldsymbol{P}^{*\top}$ yields

$$\boldsymbol{\Lambda}^2\boldsymbol{H}' - 2\boldsymbol{\Lambda}\boldsymbol{H}'\boldsymbol{\Lambda} + \boldsymbol{H}'\boldsymbol{\Lambda}^2 = 0, \qquad \operatorname{tr}\left(\boldsymbol{\Lambda}^n\boldsymbol{H}'\right) = \operatorname{tr}\left(\boldsymbol{\Omega}^n \operatorname{dev}\hat{\boldsymbol{H}}_0\right), \qquad \boldsymbol{H}' = \boldsymbol{P}^{*\top}\operatorname{dev}\hat{\boldsymbol{H}}_{\text{eq}}\boldsymbol{P}. \tag{33}$$

Rewriting the first equation from (33) in a component form, it can be shown that off-diagonal elements of matrix $\boldsymbol{H}'$ are equal to zero. The second equation from (33) is represented as

$$\sum_{j=1}^{N} \omega_j^{2n} H'_{jj} = \sum_{j=1}^{N} \omega_j^{2n} \{\boldsymbol{P}^{*\top}\operatorname{dev}\hat{\boldsymbol{H}}_0\boldsymbol{P}\}_{jj}. \tag{34}$$

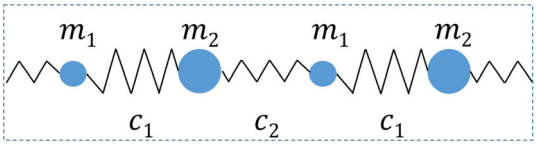

Fig. 2 Two unit cells of a diatomic chain with alternating masses and stiffness. Particles of different sizes form two sublattices

Then, the solution of Eq. (33) takes form:

$$H'_{ij} = \{\boldsymbol{P}^{*\top} \mathrm{dev} \hat{\boldsymbol{H}}_0 \boldsymbol{P}\}_{ij} \delta_{ij}. \tag{35}$$

Substitution of formula (35) into the last formula from (33) allows to calculate matrix $\hat{\boldsymbol{H}}$. Applying the inverse discrete Fourier transform and using formulas (10), (30) yields:

$$k_{\mathrm{B}} \boldsymbol{T}_{\mathrm{eq}} = \frac{1}{N} \mathrm{tr}\,(\boldsymbol{H}_0)\, \boldsymbol{E} + \int_{\mathbf{k}} \boldsymbol{P} \mathrm{diag} \left(\boldsymbol{P}^{*\top} \mathrm{dev} \hat{\boldsymbol{H}}_0 \boldsymbol{P} \right) \boldsymbol{P}^{*\top} \mathrm{d}\mathbf{k}. \tag{36}$$

In the first term, $\boldsymbol{H}_0$ is calculated at $\mathbf{x} = \mathbf{y}$.

Remark Evolution of the generalized Hamiltonian is governed by fourth-order Eq. (12). Therefore, $\boldsymbol{H}_{\mathrm{eq}}$ and $\boldsymbol{T}_{\mathrm{eq}}$, in principle, can be influenced by $\boldsymbol{H}_0$, $\dot{\boldsymbol{H}}_0$, $\ddot{\boldsymbol{H}}_0$, $\dddot{\boldsymbol{H}}_0$. However, formula (36) shows that only $\boldsymbol{H}_0$ matters.

Thus, formula (36) is a generalization of formula (27) for the case of arbitrary initial conditions. It shows that, in general, equilibrium temperatures, corresponding to different degrees of freedom of the unit cell, are not equal. Formula (36) can be referred to as *the non-equipartition theorem*. The theorem relates equilibrium temperature matrix with initial conditions.

5 Example: Diatomic chain

5.1 Equations of motion

Presented theory is applicable to crystals with an arbitrary lattice. In this section, the simplest one-dimensional polyatomic lattice is analyzed.

We consider a diatomic chain with alternating masses m_1, m_2 and stiffness c_1, c_2 (see Fig. 2). The chain consists of two *sublattices*, one formed by particles with masses m_1 and another formed by particles with masses m_2.

This model is frequently used as an example of a system with two branches of dispersion relation [11,41, 57,66].

We write equations of motion of the chain in matrix form (4). Unit cells, containing two particles each, are numbered by index j. Position vector of the jth unit cell has form $\mathbf{x}_j = j\mathbf{b}$, where $\mathbf{b}$ is a primitive vector of the lattice. Each particle has one degree of freedom. Displacements of particles, belonging to the unit cell j, form a column

$$\boldsymbol{u}_j = \boldsymbol{u}(\mathbf{x}_j) = \begin{bmatrix} u_{1j} & u_{2j} \end{bmatrix}^{\top}, \tag{37}$$

where u_{1j}, u_{2j} are displacements of particles with masses m_1 and m_2, respectively. Then, equations of motion have form

$$\begin{gathered} \boldsymbol{M}\ddot{\boldsymbol{u}}_j = \boldsymbol{C}_1 \boldsymbol{u}_{j+1} + \boldsymbol{C}_0 \boldsymbol{u}_j + \boldsymbol{C}_{-1} \boldsymbol{u}_{j-1}, \\ \boldsymbol{M} = \begin{bmatrix} m_1 & 0 \\ 0 & m_2 \end{bmatrix}, \quad \boldsymbol{C}_0 = \begin{bmatrix} -c_1 - c_2 & c_1 \\ c_1 & -c_1 - c_2 \end{bmatrix}, \quad \boldsymbol{C}_1 = \begin{bmatrix} 0 & 0 \\ c_2 & 0 \end{bmatrix}. \end{gathered} \tag{38}$$

Here, $\boldsymbol{C}_{-1} = \boldsymbol{C}_1^{\top}$.

Initially, particles have random velocities and zero displacements:

$$u_{1j} = u_{2j} = 0, \quad \dot{u}_{1j} = \beta_j \sqrt{\frac{k_{\mathrm{B}}}{m_1} T_{11}^0}, \quad \dot{u}_{2j} = \gamma_j \sqrt{\frac{k_{\mathrm{B}}}{m_2} T_{22}^0}, \tag{39}$$

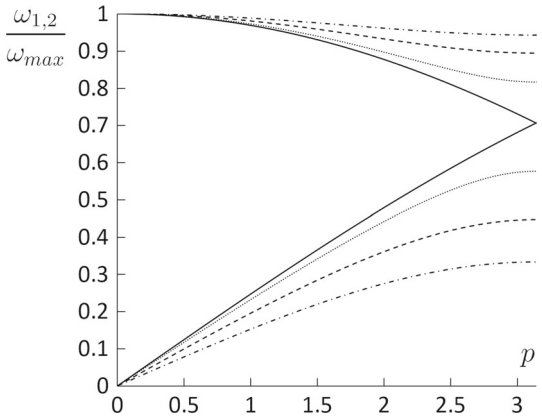

Fig. 3 Dispersion relation for a chain with alternating stiffness ($m_1 = m_2$). Curves correspond to different stiffness ratios: $\frac{c_1}{c_2} = 1$ (solid line); $\frac{1}{2}$ (dots); $\frac{1}{4}$ (dashed line); $\frac{1}{8}$ (dash-dotted line)

where T_{11}^0, T_{22}^0 are initial temperatures of sublattices, independent of j; β_j, γ_j are uncorrelated random values with zero mean and unit variance, i.e., $\langle\beta_j\rangle = \langle\gamma_j\rangle = 0$, $\langle\beta_j^2\rangle = \langle\gamma_j^2\rangle = 1$, $\langle\beta_i\gamma_j\rangle = 0$ for all i, j. Initial temperature matrix, corresponding to initial conditions (39), has the form

$$\boldsymbol{T}_0 = \begin{bmatrix} T_{11}^0 & 0 \\ 0 & T_{22}^0 \end{bmatrix}, \qquad k_B T_{11}^0 = m_1\langle\dot{u}_{1j}^2\rangle, \qquad k_B T_{22}^0 = m_2\langle\dot{u}_{2j}^2\rangle. \tag{40}$$

Here, velocities are calculated at $t = 0$. Spatial distribution of initial temperature matrix is uniform.

Further, we consider time evolution of temperatures of sublattices, equal to diagonal elements, T_{11}, T_{22}, of the temperature matrix (7).

5.2 Dispersion relation

Time evolution of temperature matrix is described by formula (22). In this section, we calculate the dispersion relation and matrix $\boldsymbol{P}$ included in this formula.

We calculate dynamical matrix, $\boldsymbol{\Omega}$, by formula (18). Substituting expressions (38) for matrices $\boldsymbol{C}_\alpha$, $\alpha = 0; \pm 1$ into formula (18), we obtain:

$$\boldsymbol{\Omega} = \begin{bmatrix} \frac{c_1+c_2}{m_1} & -\frac{c_1+c_2e^{-ip}}{\sqrt{m_1m_2}} \\ -\frac{c_1+c_2e^{ip}}{\sqrt{m_1m_2}} & \frac{c_1+c_2}{m_2} \end{bmatrix}, \qquad \mathbf{k} = p\tilde{\mathbf{b}}, \tag{41}$$

where $\mathbf{k}$ is a wave vector; $\tilde{\mathbf{b}} \cdot \mathbf{b} = 1$; $p \in [0; 2\pi]$. Calculation of eigenvalues of matrix $\boldsymbol{\Omega}$ yields the dispersion relation:

$$\omega_{1,2}^2(p) = \frac{\omega_{\max}^2}{2}\left(1 \pm \sqrt{1 - \frac{16m_1m_2c_1c_2\sin^2\frac{p}{2}}{(m_1+m_2)^2(c_1+c_2)^2}}\right), \quad \omega_{\max}^2 = \frac{(c_1+c_2)(m_1+m_2)}{m_1m_2}, \tag{42}$$

where index 1 corresponds to plus sign. Functions $\omega_1(p)$, $\omega_2(p)$ are referred to as optical and acoustic branches of the dispersion relation, respectively. Note that $\omega_{1,2}/\omega_{\max}$ equally depend on m_1/m_2 and c_1/c_2. Branches of dispersion relation for different ratios of stiffness are shown in Fig. 3.

We calculate matrix $\boldsymbol{P}$ in Eq. (22). By definition, matrix $\boldsymbol{P}$ consists of normalized eigenvectors of dynamical matrix $\boldsymbol{\Omega}$. Eigenvectors $\boldsymbol{d}_{1,2}$, corresponding to eigenvalues $\omega_{1,2}^2$ (formula (42)), have the form:

$$\boldsymbol{d}_{1,2} = \left[1 - \frac{m_1}{m_2} \pm \sqrt{\left(1 - \frac{m_1}{m_2}\right)^2 + 4|g|^2\frac{m_1}{m_2}} - 2g\sqrt{\frac{m_1}{m_2}}\right]^\top, \qquad g = \frac{c_1 + c_2e^{ip}}{c_1 + c_2}. \tag{43}$$

Normalization of vectors $\boldsymbol{d}_{1,2}$ yields columns of matrix $\boldsymbol{P}$.

In the following sections, formulas (42), (43) are employed for description of temperature oscillations and calculation of equilibrium temperatures of sublattices.

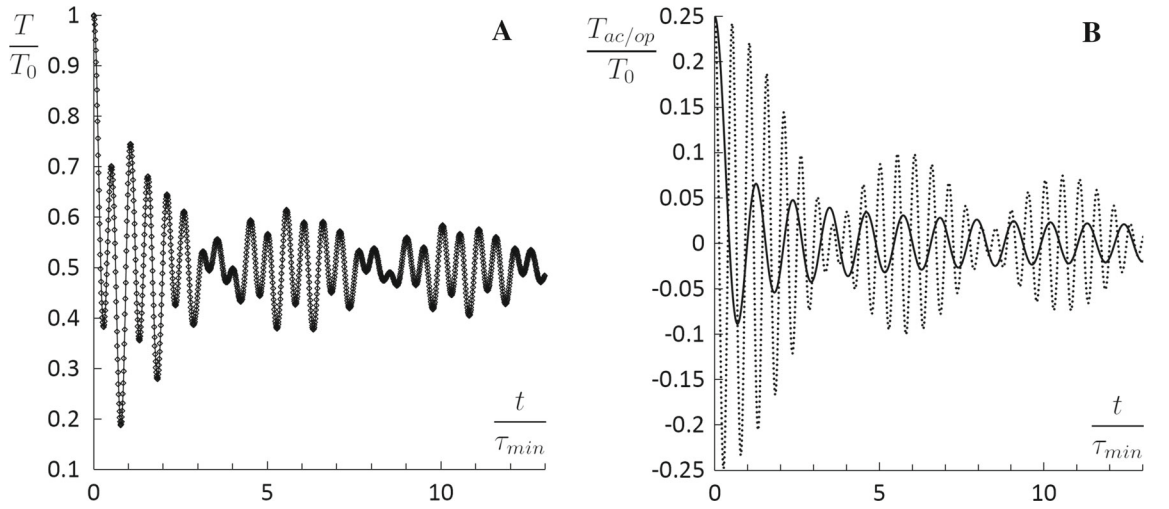

Fig. 4 **a** Oscillations of kinetic temperature ($m_2 = 4m_1$, $c_1 = c_2$). Initial temperatures of sublattices are equal. Analytical solution (44) (solid line), and numerical solution (dots). **b** Contribution of acoustic (T_{ac}, solid line) and optical (T_{op}, dots) branches to oscillations of kinetic temperature ($m_2 = 4m_1$, $c_1 = c_2$)

5.3 Oscillations of kinetic temperature

In this section, we consider oscillations of kinetic temperature $T = \frac{1}{2}(T_{11} + T_{22})$ and investigate individual contributions of acoustic and optical branches to these oscillations. The oscillations are caused by equilibration of kinetic and potential energies.

Initially, particles have random velocities and zero displacements (39). Initial kinetic energies (temperatures) of sublattices are equal ($T_{11}^0 = T_{22}^0$). The oscillations of kinetic temperature are described by formula (25). In this case, the formula reads

$$T = \frac{T_0}{2} + T_{\text{ac}} + T_{\text{op}}, \quad T_{\text{ac}} = \frac{T_0}{8\pi}\int_0^{2\pi} \cos(2\omega_2(p)t)\mathrm{d}p, \quad T_{\text{op}} = \frac{T_0}{8\pi}\int_0^{2\pi} \cos(2\omega_1(p)t)\mathrm{d}p, \tag{44}$$

where $T_0 = \frac{1}{2}\left(T_{11}^0 + T_{22}^0\right)$ is initial kinetic temperature; dispersion relation $\omega_j(p)$, $j = 1, 2$ is given by formula (42). Contributions of acoustic and optical branches to temperature oscillations are given by T_{ac}, T_{op}. In further calculations, integrals in formula (44) are evaluated numerically using Riemann sum approximation. Interval of integration is divided into 10^3 equal segments.

To check formula (44), we compare it with results of numerical solution of lattice dynamics Eq. (38) with initial conditions (39). In simulations, the chain consists of $5 \cdot 10^5$ particles under periodic boundary conditions. Numerical integration is carried out using symplectic leap-frog integrator with time step $10^{-3}\tau_{\text{min}}$, where $\tau_{\text{min}} = 2\pi/\omega_{\text{max}}$, ω_{max} is defined by formula (42). During the simulation, the total kinetic energy of the chain, proportional to kinetic temperature, is calculated. In this case, averaging over realizations is not necessary. Time dependence of temperature for $m_2/m_1 = 4$ is shown in Fig. 4a.

It is seen that analytical solution (44) practically coincides with results of numerical integration of lattice dynamics equations.

Consider contributions T_{ac}, T_{op} of two branches of dispersion relation to oscillations of kinetic temperature. Time dependencies of T_{ac}, T_{op} for $m_2 = 4m_1$, $c_1 = c_2$ are shown in Fig. 4b. It is seen that contribution of optical branch has a form of beats (two close frequencies), while contribution of acoustic branch has one main frequency. Using the stationary phase method [15], it can be shown that characteristic frequencies of temperature oscillations belong to frequency spectrum of the chain. Group velocities, corresponding to these frequencies, are equal to zero. Figure 3 shows that group velocity of acoustic waves is equal to zero for $p = \pi$, and group velocity of optical waves vanishes at $p = 0$, $p = \pi$. Then, main frequencies of temperature oscillations are the following

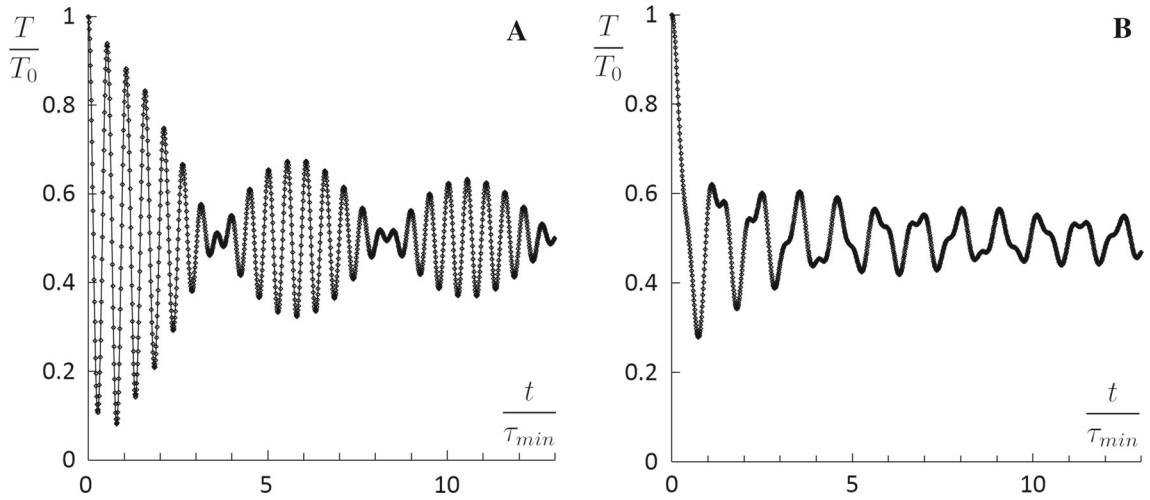

Fig. 5 Influence of initial temperatures of sublattices on temperature oscillations ($m_2 = 4m_1$, $c_1 = c_2$). Here $T_{11}^0 \neq 0$, $T_{22}^0 = 0$ (left) and $T_{11}^0 = 0$, $T_{22}^0 \neq 0$ (right). Analytical solution (25) (line), and numerical solution of lattice dynamics equations (dots)

$$\begin{aligned} &\omega_1|_{p=0} = \omega_{\max}, \qquad \omega_1^2|_{p=\pi} = \frac{\omega_{\max}^2}{2}\left(1 + \sqrt{1 - \frac{16m_1m_2c_1c_2}{(m_1+m_2)^2(c_1+c_2)^2}}\right), \\ &\omega_2^2|_{p=\pi} = \frac{\omega_{\max}^2}{2}\left(1 - \sqrt{1 - \frac{16m_1m_2c_1c_2}{(m_1+m_2)^2(c_1+c_2)^2}}\right). \end{aligned} \tag{45}$$

At large times, oscillations of kinetic temperature are represented as a sum of three harmonics with frequencies (45) and amplitudes, inversely proportional to $\sqrt{t}$. Difference between optical frequencies $\omega_1|_{p=0}$ and $\omega_1|_{p=\pi}$ decreases with increasing mass ratio, and therefore, beats of kinetic temperature are observed (see Fig. 4). Note that similar beats of temperature are observed in two-dimensional triangular lattice [62].

Consider influence of difference between initial temperatures of sublattices T_{11}^0, T_{22}^0 on temperature oscillations. The oscillations for two different cases, $T_{11}^0 \neq 0$, $T_{22}^0 = 0$ and $T_{11}^0 = 0$, $T_{22}^0 \neq 0$, are shown in Fig. 5. It is seen that the form of oscillations significantly depends on the difference between T_{11}^0 and T_{22}^0. In both cases, analytical results, obtained using formula (25), practically coincide with numerical solution of lattice dynamics equations.

Thus, temperature oscillations are accurately described by formula (25). Amplitude of the oscillations decays in time as[15] $1/\sqrt{t}$. Main frequencies of temperature oscillations belong to spectrum of the chain and correspond to zero group velocities. Form of oscillations significantly depends on initial distribution of energy between sublattices.

5.4 Redistribution of temperature between sublattices

In this section, we consider the case when initial temperatures of sublattices are not equal ($T_{11}^0 \neq T_{22}^0$). Then temperature is redistributed between the sublattices.

Numerical solution of equations of motion (38) shows that difference between temperatures of sublattices, $T_{11} - T_{22}$, tends to some equilibrium value. For example, behavior of $T_{11} - T_{22}$ for $m_2 = 4m_1$, $c_1 = c_2$ is shown in Fig. 6. Two cases $T_{11}^0 \neq 0$, $T_{22}^0 = 0$ and $T_{11}^0 = 0$, $T_{22}^0 \neq 0$ are considered.

It is seen that in both cases difference between temperatures tends to the value $0.3(T_{11}^0 - T_{22}^0)$, predicted by formula (47). Note that shape of curves for two initial conditions is different. Therefore, the process of redistribution of temperature between sublattices depends on difference between T_{11}^0 and T_{22}^0.

[15] This fact follows form the asymptotic analysis based on the stationary phase method [15].

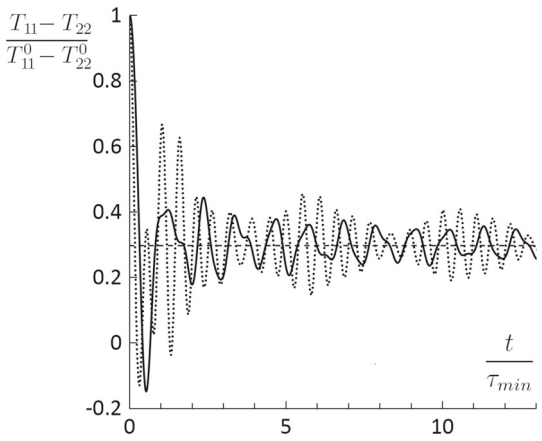

Fig. 6 Difference between temperatures of sublattices for $T_{11}^0 \neq 0$, $T_{22}^0 = 0$ (solid line), and $T_{11}^0 = 0$, $T_{22}^0 \neq 0$ (dots). Here $m_2 = 4m_1$, $c_1 = c_2$, T_{11}^0, T_{22}^0 are initial temperatures of sublattices

We calculate the difference between temperatures of sublattices at thermal equilibrium using formula (27). Deviator of initial temperature matrix has form

$$\mathrm{dev}\boldsymbol{T}_0 = \frac{T_{11}^0 - T_{22}^0}{2}\boldsymbol{I}, \qquad \boldsymbol{I} = \begin{bmatrix} 1 & 0 \\ 0 & -1 \end{bmatrix}. \tag{46}$$

Substituting (46) into formula (27) yields:

$$\boldsymbol{T}_{\mathrm{eq}} = \frac{1}{4}\left(T_{11}^0 + T_{22}^0\right)\boldsymbol{E} + \frac{T_{11}^0 - T_{22}^0}{4\pi}\int_0^{2\pi} \boldsymbol{P}\mathrm{diag}\left(\boldsymbol{P}^{*\top}\boldsymbol{I}\boldsymbol{P}\right)\boldsymbol{P}^{*\top}\mathrm{d}p. \tag{47}$$

Matrix $\boldsymbol{P}$ is given by formula (43). Formula (47) yields equilibrium temperatures of sublattices. Integral in formula (47) is calculated numerically using Riemann sum approximation. Interval of integration is divided into 10^3 equal segments.

Consider the case of equal masses $m_1 = m_2$. Using formula (43), it can be shown that diagonal elements of matrix $\boldsymbol{P}^{*\top}\boldsymbol{I}\boldsymbol{P}$ are equal to zero. Then, from formula (47) it follows that for $m_1 = m_2$ and arbitrary c_1/c_2 temperatures of sublattices at thermal equilibrium are equal.

To check formula (47), we compare it with results of numerical solution of lattice dynamics equations (38) with initial conditions (39). The chain consists of 10^4 particles under periodic boundary conditions. We limit ourselves by the following range of parameters: $m_1/m_2 \in [0; 1]$ and $c_1/c_2 \in [0; 1]$. Numerical integration is carried out with time step $10^{-3}\tau_*$, where $\tau_* = \sqrt{\frac{c_1+c_2}{m_1}}$. Initially, particles have random velocities (39) such that one of the sublattices has zero temperature. During the simulation, temperatures of sublattices are calculated. Equilibrium temperatures are computed by averaging corresponding kinetic energies over time interval $[t_{\max}/4; t_{\max}]$, where $t_{\max}$ is the total simulation time. Reasonable accuracy is achieved for $t_{\max} = 10^2\tau_*$.

Equilibrium difference between temperatures of sublattices for different mass and stiffness ratios is shown in Fig. 7. It is seen that for any given mass ratio, difference between temperatures decreases with decreasing c_1/c_2 and tends to a limiting value corresponding to the case $c_1/c_2 \to 0$. In particular, results for $c_2 = 64c_1$ and $c_2 = 32c_1$ are practically indistinguishable.

Thus for the given system, equilibrium temperatures of sublattices are equal if either (1) initial temperatures are equal $T_{11}^0 = T_{22}^0$ or (2) masses are equal $m_1 = m_2$ and stiffness ratio is arbitrary. In general, equilibrium temperatures of sublattices are different. Their values are accurately determined by the non-equipartition theorem (formula (47)).

Remark For equal stiffness $c_1 = c_2$, Eq. (38) is also valid for transverse vibrations of a stretched diatomic chain. In this case, the stiffness is determined by magnitude of stretching force. Therefore all results obtained in this section can be used in the case of transverse vibrations.

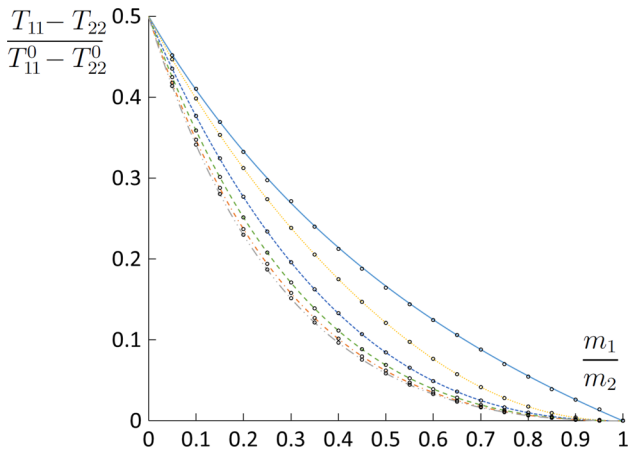

Fig. 7 Difference between equilibrium temperatures of sublattices for a diatomic chain. Here, T_{11}^0, T_{22}^0 are initial temperatures of sublattices. Curves are calculated using formula (47) for $\frac{c_1}{c_2} = 1$ (solid line); $\frac{1}{2}$ (doted line); $\frac{1}{4}$ (short dashed line); $\frac{1}{8}$ (dashed line); $\frac{1}{16}$ (dash-dotted line); $\frac{1}{32}$ (dash-double doted line). Circles correspond to results of numerical integration of equations of motion (38)

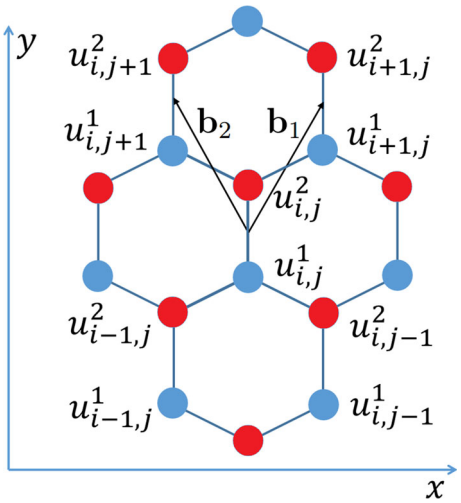

Fig. 8 Numbering of unit cells in a graphene sheet. Two sublattices are indicated by different colors. Here, $\mathbf{b}_1$, $\mathbf{b}_2$ are primitive vectors of the lattice. Particles move along the normal to lattice plane

Remark Our results may serve for better understanding of breakdown of equipartition in heat conducting diatomic chains. In papers [31,65], stationary heat transfer in diatomic chains connecting two thermal reservoirs with different temperatures was investigated. In paper [9], it was shown that for $m_1 \neq m_2$ temperatures of sublattices were different (temperature profile was not smooth), while in paper [65] temperatures of sublattices for $m_1 = m_2$ and $c_1 \neq c_2$ were practically equal. These results are consistent with prediction of formula (47), which shows that equilibrium temperatures of sublattices are equal only for $m_1 = m_2$.

6 Example. Graphene lattice (out-of-plane motions)

6.1 Equations of motion

In this section, we consider approach to thermal equilibrium in a stretched graphene lattice (see Fig. 8). Only out-of-plane vibrations are considered. In-plane vibrations can be considered separately, since in harmonic approximation in-plane and out-of-plane vibrations are decoupled.

Unit cells, containing two particles each, are numbered by a pair of indices i, j (see Fig. 8). Primitive vectors $\mathbf{b}_1$ and $\mathbf{b}_2$ for graphene have the form:

$$\mathbf{b}_1 = \frac{\sqrt{3}a}{2}\left(\mathbf{i} + \sqrt{3}\mathbf{j}\right), \qquad \mathbf{b}_2 = \frac{\sqrt{3}a}{2}\left(\sqrt{3}\mathbf{j} - \mathbf{i}\right), \tag{48}$$

where $\mathbf{i}$, $\mathbf{j}$ are Cartesian unit vectors corresponding to x and y, axes, respectively (see Fig. 8). Position vector of cell i, j is represented via the primitive vectors as $\mathbf{x}_{i,j} = i\mathbf{b}_1 + j\mathbf{b}_2$.

Each particle has one degree of freedom (displacement along normal to the lattice plane). Displacements of a unit cell i, j form a column:

$$\boldsymbol{u}_{i,j} = \boldsymbol{u}(\mathbf{x}_{i,j}) = \begin{bmatrix} u^1_{i,j} & u^2_{i,j} \end{bmatrix}^\top, \tag{49}$$

where $u^1_{i,j}$, $u^2_{i,j}$ are displacements of two sublattices.

Consider equations of motion of unit cell i, j. Each particle is connected with three nearest neighbors by linear springs (solid lines in Fig. 8). Equilibrium length of the spring is less than initial distance between particles, i.e., the graphene sheet is uniformly stretched.[16] Then, equations of motion have the form

$$\begin{gathered} \boldsymbol{M}\ddot{\boldsymbol{u}}_{i,j} = \boldsymbol{C}_1\boldsymbol{u}_{i+1,j} + \boldsymbol{C}_{-1}\boldsymbol{u}_{i-1,j} + \boldsymbol{C}_0\boldsymbol{u}_{i,j} + \boldsymbol{C}_2\boldsymbol{u}_{i,j+1} + \boldsymbol{C}_{-2}\boldsymbol{u}_{i,j-1}, \\ \boldsymbol{M} = \begin{bmatrix} m & 0 \\ 0 & m \end{bmatrix}, \quad \boldsymbol{C}_0 = \begin{bmatrix} -3c & c \\ c & -3c \end{bmatrix}, \quad \boldsymbol{C}_1 = \boldsymbol{C}_2 = \begin{bmatrix} 0 & 0 \\ c & 0 \end{bmatrix}. \end{gathered} \tag{50}$$

Here, $\boldsymbol{C}_{-1} = \boldsymbol{C}_1^\top$, $\boldsymbol{C}_{-2} = \boldsymbol{C}_2^\top$; m is particle mass; c is stiffness, depending on initial tension of a sheet. The given model can be used for description of out-of-plane vibrations of a stretched graphene sheet [3,6,20].

Initially, particles have random velocities and zero displacements:

$$u^1_{i,j} = u^2_{i,j} = 0, \quad \dot{u}^1_{i,j} = \beta_{i,j}\sqrt{\frac{k_\mathrm{B}}{m}T^0_{11}}, \quad \dot{u}^2_{i,j} = \gamma_{i,j}\sqrt{\frac{k_\mathrm{B}}{m}T^0_{22}}, \tag{51}$$

where T^0_{11}, T^0_{22} are temperatures of sublattices, independent of i, j; $\beta_{i,j}$, $\gamma_{i,j}$ are uncorrelated random values with zero mean and unit variance, i.e., $\left\langle \beta_{i,j} \right\rangle = \left\langle \gamma_{i,j} \right\rangle = 0$, $\left\langle \beta^2_{i,j} \right\rangle = \left\langle \gamma^2_{i,j} \right\rangle = 1$, $\left\langle \beta_{i,j}\gamma_{s,p} \right\rangle = 0$ for all i, j, s, p. Initial temperature matrix, $\boldsymbol{T}_0$, corresponding to initial conditions (51), has form:

$$\boldsymbol{T}_0 = \begin{bmatrix} T^0_{11} & 0 \\ 0 & T^0_{22} \end{bmatrix}, \qquad k_\mathrm{B}T^0_{11} = m\left\langle \left(\dot{u}^1_{i,j}\right)^2 \right\rangle, \qquad k_\mathrm{B}T^0_{22} = m\left\langle \left(\dot{u}^2_{i,j}\right)^2 \right\rangle. \tag{52}$$

Here, velocities are calculated at $t = 0$. Spatial distribution of initial temperature matrix is uniform.

Further, we consider time evolution of temperatures of sublattices, equal to diagonal elements T_{11}, T_{22} of the temperature matrix.

6.2 Dispersion relation

Evolution of temperature matrix during approach to thermal equilibrium is described by formula (22). In this section, we calculate the dispersion relation and matrix $\boldsymbol{P}$ included in this formula.

We calculate dynamical matrix $\boldsymbol{\Omega}$ using formula (18). Substituting expressions (50) for matrices $\boldsymbol{C}_\alpha$, $\alpha = 0; \pm 1; \pm 2$ into formula (18), we obtain:

$$\boldsymbol{\Omega} = \omega_*^2 \begin{bmatrix} 3 & -1 - e^{-\mathrm{i}p_1} - e^{-\mathrm{i}p_2} \\ -1 - e^{\mathrm{i}p_1} - e^{\mathrm{i}p_2} & 3 \end{bmatrix}, \qquad p_1 = \mathbf{k}\cdot\mathbf{b}_1, \quad p_2 = \mathbf{k}\cdot\mathbf{b}_2, \tag{53}$$

where $\mathbf{k}$ is wave vector; $\omega_*^2 = \frac{c}{m}$; p_1, $p_2 \in [0; 2\pi]$ are dimensionless components of the wave vector.

Eigenvalues ω_1^2, ω_2^2 of matrix $\boldsymbol{\Omega}$ determine dispersion relation for the lattice. Solution of the eigenvalue problem yields:

[16] In the absence of stretching, out-of-plane vibrations are essentially nonlinear. Various nonlinear effects in unstrained graphene are considered, e.g., in papers [4,33].

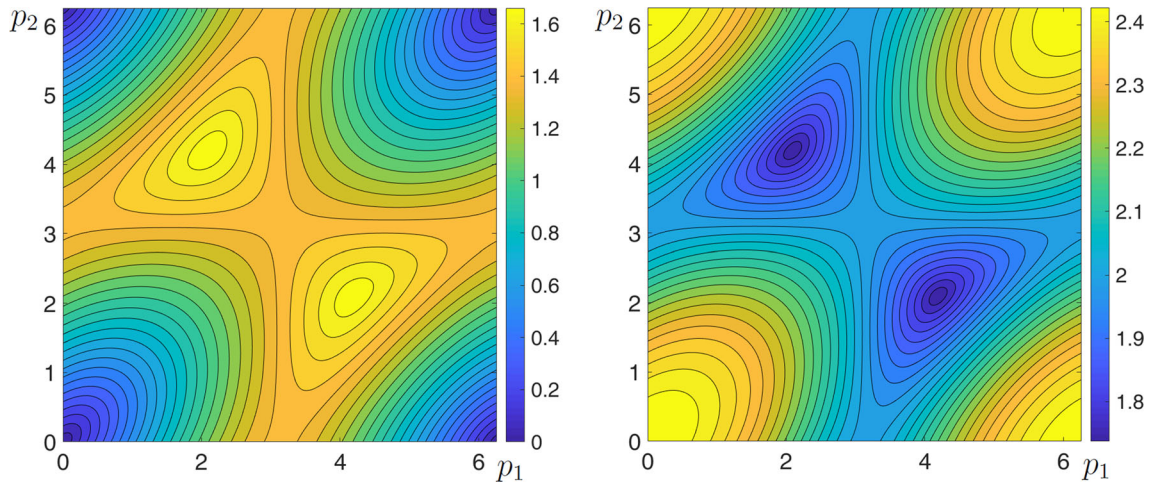

Fig. 9 Acoustic ($\omega_2(p_1, p_2)/\omega_*$, left) and optical ($\omega_1(p_1, p_2)/\omega_*$, right) dispersion surfaces (54) for out-of-plane vibrations of graphene

$$\omega_{1,2}^2 = \omega_*^2 \left(3 \pm \sqrt{3 + 2\left(\cos p_1 + \cos p_2 + \cos\left(p_1 - p_2\right)\right)}\right), \tag{54}$$

where index 1 corresponds to plus sign. Functions $\omega_1(p_1, p_2), \omega_2(p_1, p_2)$ are referred to as optical and acoustic dispersion surfaces, respectively (see Fig. 9).

Eigenvectors of matrix $\boldsymbol{\Omega}$ are columns of matrix $\boldsymbol{P}$:

$$\boldsymbol{P} = \frac{1}{\sqrt{|g|^2 + g^2}} \begin{bmatrix} |g| & |g| \\ -g & g \end{bmatrix}, \qquad g = 1 + e^{\mathrm{i}p_1} + e^{\mathrm{i}p_2}. \tag{55}$$

In the following sections, formulas (53), (54), (55) are employed for description of temperature oscillations and calculation of equilibrium temperatures of sublattices.

6.3 Oscillations of kinetic temperature

In this section, we consider oscillations of kinetic temperature $T = \frac{1}{2}(T_{11} + T_{22})$ in graphene.

In general, the oscillations are described by formula (24). Using formulas (52), (55), it can be shown that diagonal elements of matrix $\boldsymbol{P}^{*\top} \mathrm{dev} \boldsymbol{T}_0 \boldsymbol{P}$ are equal to zero. Then, from formula (24) it follows that temperature oscillations are independent of difference between temperatures of sublattices T_{11}^0 and T_{22}^0. Then, formula (25) can be used:

$$\begin{aligned} T &= \frac{T_0}{2} + T_{\mathrm{ac}} + T_{\mathrm{op}}, \qquad T_{\mathrm{ac}} = \frac{T_0}{16\pi^2} \int_0^{2\pi} \int_0^{2\pi} \cos(2\omega_2(p_1, p_2)t)\mathrm{d}p_1\mathrm{d}p_2, \\ T_{\mathrm{op}} &= \frac{T_0}{16\pi^2} \int_0^{2\pi} \int_0^{2\pi} \cos(2\omega_1(p_1, p_2)t)\mathrm{d}p_1\mathrm{d}p_2, \end{aligned} \tag{56}$$

where $T_0 = \frac{1}{2}\left(T_{11}^0 + T_{22}^0\right)$ is initial kinetic temperature; functions $\omega_{1,2}(p_1, p_2)$ are given by formula (54). In further calculations, integrals in formula (56) are evaluated using Riemann sum approximation. Integration area is divided into 400×400 equal square elements.

To check formula (56), we compare it with results of numerical solution of lattice dynamics equations (50) with initial conditions (51). In our simulations, graphene sheet contains $10^3 \times 10^3$ unit cells under periodic boundary conditions. Numerical integration is carried out with time step $5 \cdot 10^{-3}\tau_*$, where $\tau_* = 2\pi/\omega_*$. During the simulation, the total kinetic energy of the lattice, proportional to kinetic temperature, is calculated. In this case, averaging over realizations is not necessary. Time dependence of temperature is presented in Fig. 10a.

The figure shows that formula (56) accurately describes temperature oscillations. Calculations with different initial temperatures of sublattices ($T_{11}^0 \neq T_{22}^0$) confirm out conclusion that the ratio of these temperatures does not influence the behavior of T.

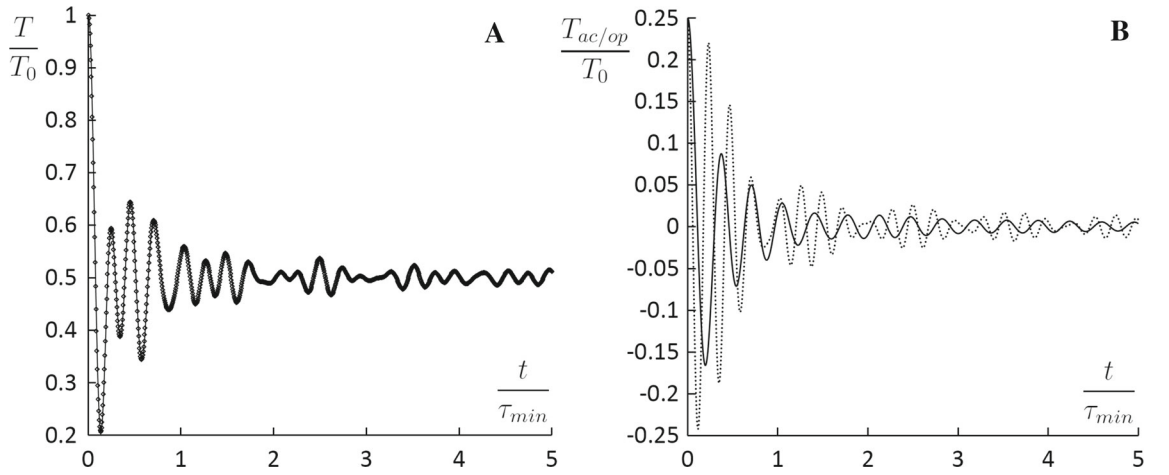

Fig. 10 **a** Oscillations of kinetic temperature in graphene sheet with random initial velocities and zero displacements. Numerical solution of equations of motion (50) (dots) and analytical solution (56) (line). **b** Contribution of acoustic (T_{ac}, solid line) and optical (T_{op}, dotted line) dispersion surfaces to temperature oscillations in graphene

Contributions of acoustic and optical dispersion surfaces to temperature oscillations are shown in Fig. 10b. The contributions are given by integrals T_{ac} and T_{op} (formula (56)). It is seen that oscillations corresponding to optical dispersion surface have two main frequencies, while oscillations corresponding to acoustic surface have only one main frequency. The frequencies can be calculated using asymptotic analysis of integrals (56) at large t using the stationary phase method [15]. This investigation is beyond the scope of the present paper. Similar investigation for two-dimensional triangular lattice is carried out in paper [62].

Thus, oscillations of kinetic temperature are accurately described by formula (56). Amplitude of these oscillations decays in time as $1/t$. Formula (56) is valid for an arbitrary ratio of initial temperatures of sublattices.

6.4 Redistribution of temperature between sublattices

In this section, we consider redistribution of kinetic temperature between sublattices in graphene in the case $T_{11}^0 \neq T_{22}^0$.

Equilibrium temperatures of sublattices are calculated using formula (27). Corresponding expression for initial temperature matrix is given by formula (52). In the previous section, it is mentioned that for graphene, matrix $\boldsymbol{P}^{*\top}\operatorname{dev}\boldsymbol{T}_0\boldsymbol{P}$ in formula (27) has zero diagonal elements. Then, from formula (27) it follows that $\operatorname{dev}\boldsymbol{T}_{\text{eq}} = 0$, i.e., temperatures of sublattices equilibrate.

To check this fact, consider numerical solution of equations of motion (50) with initial conditions (51). Periodic cell containing $10^3 \times 10^3$ unit cells is used. Initially, particles of one sublattice have random velocities, while particles of another sublattice are motionless. Initial displacements are equal to zero. Numerical integration is carried with time step $5 \cdot 10^{-3}\tau_*$, where $\tau_* = 2\pi/\omega_*$. Time evolution of temperature difference, $T_{11} - T_{22}$, is shown in Fig. 11.

The figure shows beats of difference between temperatures of sublattices. The amplitude of beats decays in time as $1/t$.

Thus at large times, temperatures of sublattices in graphene become equal.

7 Conclusions

An analytical description of thermal equilibration in infinite harmonic crystals was presented.

Initially, the crystal is in a nonequilibrium state such that kinetic and potential energies are not equal. The crystal tends to thermal equilibrium, i.e., to a state in which temperatures, corresponding to different degrees of freedom of the unit cell, are constant in time. Approach to thermal equilibrium is accompanied by high-frequency oscillations of the temperatures *exactly* described by formula (22). The oscillations are caused

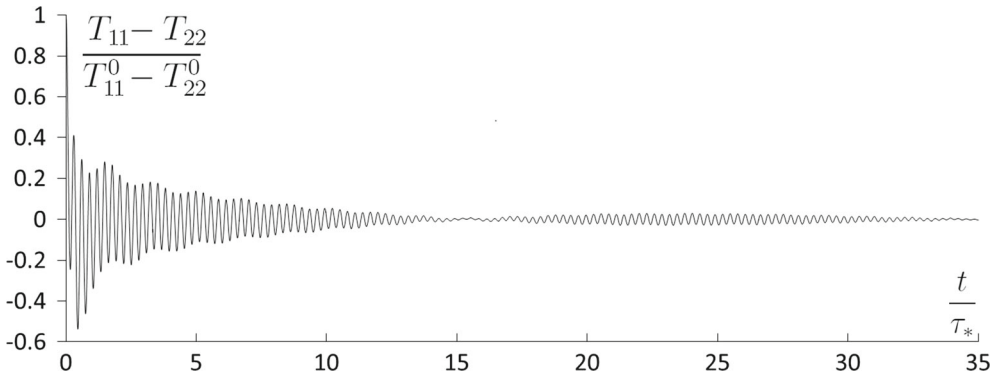

Fig. 11 Redistribution of kinetic temperatures between sublattices in graphene (numerical solution of lattice dynamics equations (50))

by two physical processes: (1) equilibration of kinetic and potential energies, and (2) redistribution of kinetic energy (temperature) among degrees of freedom of the unit cell. In d-dimensional crystal, amplitude of the oscillations decays in time as $1/t^{\frac{d}{2}}$.

At large times, kinetic and potential energies equilibrate. Kinetic energy is redistributed between degrees of freedom of the unit cell. Equilibrium values of kinetic temperatures, corresponding to different degrees of freedom of the unit cell, are related with initial conditions by *the non-equipartition theorem* (formulas (27), (36)). The theorem shows that these kinetic temperatures are equal at thermal equilibrium if their initial values are equal. If initially the kinetic temperatures are different, then they are usually different at equilibrium, except for some lattices. For example, it is shown that in diatomic chain with alternating stiffness (equal masses) and graphene lattice (out-of-plane motions) equilibrium values of the kinetic temperatures are equal.

Our analytical results are exact in the case of spatially uniform distribution of kinetic temperatures. In the case of nonuniform temperature profile, ballistic heat transport should be considered along with transient processes described above. However, the heat transport is much slower than the transient processes [18,38, 39,44,45,60]. Therefore at short times, the crystal locally almost achieve thermal equilibrium. At each spatial point, temperature matrix tends to the value predicted by the non-equipartition theorem. This fast, transient process is described by the presented theory with high accuracy. Further, slow changes in the temperature matrix are caused by ballistic heat transport. We refer to papers [44,45] for detailed analysis of the nonuniform case.

In the present paper, anharmonic effects were neglected. Anharmonicity leads, in particular, to exchange of energy between normal modes. In this case, temperatures, corresponding to different degrees of freedom of the unit cell, tend to equal equilibrium values. However in papers [5,43,51], it is shown that, at least in the case of small anharmonicity, the exchange between normal modes is significantly slower than transient thermal processes described above. Therefore at short times, transient thermal processes in anharmonic crystals are well described by harmonic approximation [43].

In the present paper, we focused on behavior of the main observable, notably kinetic temperature (or more generally, temperature matrix). We believe that calculation of other thermodynamic quantities, such as entropy, during approach to thermal equilibrium would be an interesting extension of the present work. We refer to a recent paper [40] for detailed discussion of some issues related to calculation of entropy for harmonic crystals.

Acknowledgements The author is deeply grateful to A.M. Krivtsov, S.V. Dmitriev, M.A. Guzev, D.A. Indeitsev, E.A. Ivanova, S.N. Gavrilov, I.E. Berinskii, and A.S. Murachev for useful discussions. The work was financially supported by the Russian Science Foundation under Grant No. 17-71-10213.

Appendix I: Equation for the generalized energies

In this appendix, we show that generalized energies satisfy differential–difference equation (12).
We introduce matrix, $\boldsymbol{Z}$, consisting of covariances of particle accelerations:

$$\boldsymbol{Z} = \frac{1}{2}\boldsymbol{M}^{\frac{1}{2}}\left\langle \ddot{\boldsymbol{u}}(\mathbf{x})\ddot{\boldsymbol{u}}(\mathbf{y})^{\top}\right\rangle \boldsymbol{M}^{\frac{1}{2}}. \tag{57}$$

Calculation of the second time derivatives of generalized kinetic energy, $\boldsymbol{K}$, and $\boldsymbol{Z}$ taking into account equations of motion, yields:

$$\begin{aligned}
&\ddot{\boldsymbol{K}} = \mathcal{L}_x \boldsymbol{K} + \boldsymbol{K}\mathcal{L}_y^\top + 2\boldsymbol{Z}, \qquad \ddot{\boldsymbol{Z}} = \mathcal{L}_x \boldsymbol{Z} + \boldsymbol{Z}\mathcal{L}_y^\top + 2\mathcal{L}_x \boldsymbol{K}\mathcal{L}_y^\top, \\
&\mathcal{L}_x \boldsymbol{K} = \sum_\alpha \boldsymbol{M}^{-\frac{1}{2}} \boldsymbol{C}_\alpha \boldsymbol{M}^{-\frac{1}{2}} \boldsymbol{K}\left(\mathbf{x}+\mathbf{a}_\alpha, \mathbf{y}\right), \quad \boldsymbol{K}\mathcal{L}_y^\top = \sum_\alpha \boldsymbol{K}\left(\mathbf{x}, \mathbf{y}+\mathbf{a}_\alpha\right) \boldsymbol{M}^{-\frac{1}{2}} \boldsymbol{C}_\alpha^\top \boldsymbol{M}^{-\frac{1}{2}}.
\end{aligned} \tag{58}$$

Excluding $\boldsymbol{Z}$ from this system of equations, we obtain

$$\dddot{\boldsymbol{K}} - 2\left(\mathcal{L}_x \ddot{\boldsymbol{K}} + \ddot{\boldsymbol{K}}\mathcal{L}_y^\top\right) + \mathcal{L}_x^2 \boldsymbol{K} - 2\mathcal{L}_x \boldsymbol{K}\mathcal{L}_y^\top + \boldsymbol{K}\left(\mathcal{L}_y^\top\right)^2 = 0, \tag{59}$$

where $\mathcal{L}_x^2 = \mathcal{L}_x \mathcal{L}_x$. Formula (59) exactly determines evolution of the generalized kinetic energy for *any* initial conditions. In particular, it can be used for description of ballistic heat transport [44].

We consider initial conditions (5), corresponding to spatially uniform temperature distribution. In this case, the following identity is satisfied $\boldsymbol{K}(\mathbf{x}, \mathbf{y}) = \boldsymbol{K}(\mathbf{x}-\mathbf{y})$. Using the identity we show that

$$\mathcal{L}_x \boldsymbol{K} = \mathcal{L}\boldsymbol{K}, \quad \boldsymbol{K}\mathcal{L}_y^\top = \boldsymbol{K}\mathcal{L}, \quad \mathcal{L}\boldsymbol{K} \stackrel{\text{def}}{=} \sum_\alpha \boldsymbol{M}^{-\frac{1}{2}} \boldsymbol{C}_\alpha \boldsymbol{M}^{-\frac{1}{2}} \boldsymbol{K}\left(\mathbf{x}-\mathbf{y}+\mathbf{a}_\alpha\right). \tag{60}$$

Substitution of expressions (60) for operators into Eq. (59) yields equation (12):

$$\dddot{\boldsymbol{K}} - 2\left(\mathcal{L}\ddot{\boldsymbol{K}} + \ddot{\boldsymbol{K}}\mathcal{L}\right) + \mathcal{L}^2 \boldsymbol{K} - 2\mathcal{L}\boldsymbol{K}\mathcal{L} + \boldsymbol{K}\mathcal{L}^2 = 0. \tag{61}$$

We introduce generalized potential energy, $\boldsymbol{\Pi}(\mathbf{x}, \mathbf{y})$, generalized Hamiltonian, $\boldsymbol{H}(\mathbf{x}, \mathbf{y})$, and generalized Lagrangian, $\boldsymbol{L}(\mathbf{x}, \mathbf{y})$:

$$\begin{aligned}
&\boldsymbol{H} = \boldsymbol{K} + \boldsymbol{\Pi}, \qquad \boldsymbol{L} = \boldsymbol{K} - \boldsymbol{\Pi}, \qquad \boldsymbol{\Pi} = -\frac{1}{4}\left(\mathcal{L}_x \boldsymbol{D} + \boldsymbol{D}\mathcal{L}_y^{\mathrm{T}}\right), \\
&\boldsymbol{D} = \boldsymbol{M}^{\frac{1}{2}} \left\langle \boldsymbol{u}(\mathbf{x}) \boldsymbol{u}(\mathbf{y})^{\mathrm{T}} \right\rangle \boldsymbol{M}^{\frac{1}{2}}.
\end{aligned} \tag{62}$$

Here, $\boldsymbol{K} = \boldsymbol{K}(\mathbf{x}, \mathbf{y})$; operators $\mathcal{L}_x$, $\mathcal{L}_y$ are defined by formula (58).

To derive equations for $\boldsymbol{\Pi}$, $\boldsymbol{L}$, and $\boldsymbol{H}$, we consider equation for $\boldsymbol{D}$. Calculation of the second time derivatives of $\boldsymbol{D}$ and $\boldsymbol{K}$ yields

$$\ddot{\boldsymbol{K}} = \mathcal{L}_x \boldsymbol{K} + \boldsymbol{K}\mathcal{L}_y^\top + \mathcal{L}_x \boldsymbol{D}\mathcal{L}_y^\top, \qquad \ddot{\boldsymbol{D}} = \mathcal{L}_x \boldsymbol{D} + \boldsymbol{D}\mathcal{L}_y^\top + 4\boldsymbol{K}. \tag{63}$$

Excluding $\boldsymbol{K}$ from this system, we obtain equation for $\boldsymbol{D}$:

$$\dddot{\boldsymbol{D}} - 2\left(\mathcal{L}_x \ddot{\boldsymbol{D}} + \ddot{\boldsymbol{D}}\mathcal{L}_y^\top\right) + \mathcal{L}_x^2 \boldsymbol{D} - 2\mathcal{L}_x \boldsymbol{D}\mathcal{L}_y^\top + \boldsymbol{D}\left(\mathcal{L}_y^\top\right)^2 = 0. \tag{64}$$

Additionally, from formula (63) it also follows that

$$\boldsymbol{L} = \frac{1}{4}\ddot{\boldsymbol{D}}. \tag{65}$$

Thus, $\boldsymbol{K}$ and $\boldsymbol{D}$ satisfy the same linear equation (64). Since generalized Hamiltonian, $\boldsymbol{H}$, and generalized Lagrangian, $\boldsymbol{L}$, are linear functions of $\boldsymbol{K}$ and $\boldsymbol{D}$, they satisfy Eq. (64). Trace of the generalized Hamiltonian is constant in time. Therefore, $\operatorname{dev}\boldsymbol{H}$ also satisfies Eq. (64).

Appendix II: Dispersion relation

In this appendix, the dispersion relation for a lattice, described by equations of motion (4), is derived.

We introduce new variable $\boldsymbol{U}(\mathbf{x}) = \boldsymbol{M}^{\frac{1}{2}}\boldsymbol{u}(\mathbf{x})$, and then, equation of motion (4) takes the form

$$\ddot{\boldsymbol{U}}(\mathbf{x}) = \sum_{\alpha} \boldsymbol{M}^{-\frac{1}{2}}\boldsymbol{C}_{\alpha}\boldsymbol{M}^{-\frac{1}{2}}\boldsymbol{U}(\mathbf{x}+\mathbf{a}_{\alpha}), \tag{66}$$

where $\boldsymbol{M}^{-\frac{1}{2}}\boldsymbol{M}^{-\frac{1}{2}} = \boldsymbol{M}^{-1}$.

The dispersion relation is derived by making substitution $\boldsymbol{U} = \boldsymbol{A}e^{\mathrm{i}(\omega t+\mathbf{k}\cdot\mathbf{x})}$ in formula (66):

$$\left(\boldsymbol{\Omega} - \omega^2\boldsymbol{E}\right)\boldsymbol{A} = 0, \qquad \boldsymbol{\Omega} = -\sum_{\alpha} \boldsymbol{M}^{-\frac{1}{2}}\boldsymbol{C}_{\alpha}\boldsymbol{M}^{-\frac{1}{2}}e^{\mathrm{i}\mathbf{k}\cdot\mathbf{a}_{\alpha}}, \tag{67}$$

where $\boldsymbol{E}$ is identity matrix; $\boldsymbol{\Omega}$ is referred to as the dynamical matrix [11]. Formula (67) yields a homogeneous system of linear equations with respect to $\boldsymbol{A}$. The system has nontrivial solution if the following condition is satisfied:

$$\det\left(\boldsymbol{\Omega}(\mathbf{k}) - \omega^2\boldsymbol{E}\right) = 0. \tag{68}$$

Here, det(...) stands for determinant of a matrix. Solutions of Eq. (68) are branches of dispersion relation $\omega_j^2(\mathbf{k})$, $j = 1, \ldots, N$. Note that from mathematical point of view, ω_j^2 are eigenvalues of $\boldsymbol{\Omega}$.

We show that dynamical matrix is Hermitian, i.e., it is equal to its own conjugate transpose:

$$\boldsymbol{\Omega}^{*\top} = -\sum_{\alpha} \boldsymbol{M}^{-\frac{1}{2}}\boldsymbol{C}_{\alpha}^{\top}\boldsymbol{M}^{-\frac{1}{2}}e^{-\mathrm{i}\mathbf{k}\cdot\mathbf{a}_{\alpha}} = -\sum_{\alpha} \boldsymbol{M}^{-\frac{1}{2}}\boldsymbol{C}_{-\alpha}\boldsymbol{M}^{-\frac{1}{2}}e^{\mathrm{i}\mathbf{k}\cdot\mathbf{a}_{-\alpha}} = \boldsymbol{\Omega}, \tag{69}$$

where identities $\mathbf{a}_{\alpha} = -\mathbf{a}_{-\alpha}$, $\boldsymbol{C}_{-\alpha} = \boldsymbol{C}_{\alpha}^{\top}$ were used.

The fact that dynamical matrix is Hermitian has two important consequences. Firstly, any Hermitian matrix, $\boldsymbol{\Omega}$, can be represented via diagonal matrix $\boldsymbol{\Lambda}$ and unitary matrix $\boldsymbol{P}$ as $\boldsymbol{\Omega} = \boldsymbol{P}\boldsymbol{\Lambda}\boldsymbol{P}^{*\top}$ (see formula (20)). Secondly, eigenvalues of Hermitian matrices are real. Therefore eigenvalues, ω_j^2, of the dynamical matrix are also real. This is a necessary, but not sufficient, condition for stability of the lattice.

Appendix III: Additional conservation laws for the generalized Hamiltonian

In this appendix, we show that the generalized Hamiltonian, $\boldsymbol{H}$, satisfies additional conservation laws. Calculating time derivative of the generalized Hamiltonian in formula (62) taking into account equations of motion yields:

$$\dot{\boldsymbol{H}} = \frac{1}{4}\left(\mathcal{L}_x\boldsymbol{W} - \boldsymbol{W}\mathcal{L}_y^{\mathrm{T}}\right), \qquad \boldsymbol{W} = \boldsymbol{M}^{\frac{1}{2}}\Big\langle\boldsymbol{u}(\mathbf{x})\boldsymbol{v}(\mathbf{y})^{\mathrm{T}} - \boldsymbol{v}(\mathbf{x})\boldsymbol{u}(\mathbf{y})^{\mathrm{T}}\Big\rangle\boldsymbol{M}^{\frac{1}{2}}. \tag{70}$$

In the case of spatially uniform initial conditions, $\boldsymbol{W} = \boldsymbol{W}(\mathbf{x}-\mathbf{y})$ and $\mathcal{L}_x\boldsymbol{W} = \mathcal{L}\boldsymbol{W}$, $\boldsymbol{W}\mathcal{L}_y^{\mathrm{T}} = \boldsymbol{W}\mathcal{L}$. Then,

$$\dot{\boldsymbol{H}} = \frac{1}{4}\left(\mathcal{L}\boldsymbol{W} - \boldsymbol{W}\mathcal{L}\right). \tag{71}$$

Multiplying Eq. (71) by $\mathcal{L}^n$, calculating trace and using identity $\mathrm{tr}\,(\boldsymbol{A}\boldsymbol{B}) = \mathrm{tr}\,(\boldsymbol{B}\boldsymbol{A})$, yields conservation laws

$$\mathrm{tr}\left(\mathcal{L}^n\boldsymbol{H}\right) = \mathrm{tr}\left(\mathcal{L}^n\boldsymbol{H}_0\right), \qquad n = 0, 1, 2, \ldots, \tag{72}$$

where $\boldsymbol{H}_0$ is initial value of the generalized Hamiltonian. For $n = 0$ and $\mathbf{x} = \mathbf{y}$, formula (72) corresponds to conventional law of energy conservation.

Formula (72) can be written for trace and deviator of the generalized Hamiltonian:

$$\mathrm{tr}\boldsymbol{H} = \mathrm{tr}\boldsymbol{H}_0, \qquad \mathrm{tr}\left(\mathcal{L}^n\mathrm{dev}\boldsymbol{H}\right) = \mathrm{tr}\left(\mathcal{L}^n\mathrm{dev}\boldsymbol{H}_0\right), \qquad n = 0, 1, 2\ldots \tag{73}$$

Conservation laws, similar to formula (72), have been derived for a one-dimensional chain in paper [7] and for two- and three-dimensional monoatomic crystals in paper [43].

References

1. Allen, M.P., Tildesley, D.J.: Computer Simulation of Liquids, p. 385. Clarendon Press, Oxford (1987)
2. Babenkov, M.B., Krivtsov, A.M., Tsvetkov, D.V.: Energy oscillations in 1D harmonic crystal on elastic foundation. Phys. Mesomech. **19**(1), 60–67 (2016)
3. Balandin, A.A.: Thermal properties of graphene and nanostructured carbon materials. Nat. Mater. **10**, 569 (2011)
4. Barani, E., Lobzenko, I.P., Korznikova, E.A., Soboleva, E.G., Dmitriev, S.V., Zhou, K., Marjaneh, A.M.: Transverse discrete breathers in unstrained graphene. Eur. Phys. J. B **90**(3), 1 (2017)
5. Benettin, G., Lo Vecchio, G., Tenenbaum, A.: Stochastic transition in two-dimensional Lennard–Jones systems. Phys. Rev. A **22**, 1709 (1980)
6. Berinskii, I.E., Krivtsov, A.M.: Linear oscillations of suspended graphene. In: Altenbach, H., Mikhasev, G. (eds.) Shell and Membrane Theories in Mechanics and Biology. Advanced Structured Materials, vol. 45. Springer, Berlin (2015)
7. Boldrighini, C., Pellegrinotti, A., Triolo, L.: Convergence to stationary states for infinite harmonic systems. J. Stat. Phys. **30**(1), 123–155 (1983)
8. Casas-Vazquez, J., Jou, D.: Temperature in non-equilibrium states: a review of open problems and current proposals. Rep. Prog. Phys. **66**, 1937–2023 (2003)
9. Casher, A., Lebowitz, J.L.: Heat flow in regular and disordered harmonic chains. J. Math. Phys. **12**, 1701 (1971)
10. Chang, A.Y., Cho, Y.-J., Chen, K.-C., Chen, C.-W., Kinaci, A., Diroll, B.T., Wagner, M.J., Chan, M.K.Y., Lin, H.-W., Schaller, R.D.: Slow organic-to-inorganic sub-lattice thermalization in methylammonium lead halide perovskites observed by ultrafast photoluminescence. Adv. Energy Mater. **6**, 1600422 (2016)
11. Dove, M.T.: Introduction to Lattice Dynamics. Cambridge University Press, London (1993)
12. Dobrushin, R.L., Pellegrinotti, A., Suhov, Y.M., Triolo, L.: One-dimensional harmonic lattice caricature of hydrodynamics. J. Stat. Phys. **43**, 3 (1986)
13. Dudnikova, T.V., Komech, A.I., Spohn, H.: On the convergence to statistical equilibrium for harmonic crystals. J. Math. Phys. **44**, 2596 (2003)
14. Dudnikova, T.V., Komech, A.I.: On the convergence to a statistical equilibrium in the crystal coupled to a scalar field. Russ. J. Math. Phys. **12**(3), 301–325 (2005)
15. Fedoryuk, M.V.: The stationary phase method and pseudodifferential operators. Russ. Math. Surv. **6**(1), 65–115 (1971)
16. Guo, P., Gong, J., Sadasivam, S., Xia, Y., Song, T.-B., Diroll, B.T., Stoumpos, C.C., Ketterson, J.B., Kanatzidis, M.G., Chan, M.K.Y., Darancet, P., Xu, T., Schaller, R.D.: Slow thermal equilibration in methylammonium lead iodide revealed by transient mid-infrared spectroscopy. Nat. Commun. **9**, 2792 (2018)
17. Guzev, M.A.: The exact formula for the temperature of a one-dimensional crystal. Dal'nevost. Mat. Zh. **18**, 39 (2018)
18. Gavrilov, S.N., Krivtsov, A.M., Tsvetkov, D.V.: Heat transfer in a one-dimensional harmonic crystal in a viscous environment subjected to an external heat supply. Cont. Mech. Thermodyn. **31**(1), 255–272 (2019)
19. Harris, L., Lukkarinen, J., Teufel, S., Theil, F.: Energy transport by acoustic modes of harmonic lattices. SIAM J. Math. Anal. **40**(4), 1392 (2008)
20. Hizhnyakov, V., Klopov, M., Shelkan, A.: Transverse intrinsic localized modes in monoatomic chain and in graphene. Phys. Lett. A **380**(9–10), 1075–1081 (2016)
21. van Hemmen, J.L.: A generalized equipartition theorem. Phys. Lett. **79A**, 1 (1980)
22. Hemmer, P.C.: Dynamic and Stochastic Types of Motion in the Linear Chain. Norges tekniske hoiskole, Trondheim (1959)
23. Holian, B.L., Hoover, W.G., Moran, B., Straub, G.K.: Shock-wave structure via nonequilibrium molecular dynamics and Navier–Stokes continuum mechanics. Phys. Rev. A **22**, 2798 (1980)
24. Holian, B.L., Mareschal, M.: Heat-flow equation motivated by the ideal-gas shock wave. Phys. Rev. E **82**, 026707 (2010)
25. Hoover, W.G.: Computational Statistical Mechanics, p. 330. Elsevier, New York (1991)
26. Hoover, W.G., Hoover, C.G., Travis, K.P.: Shock-wave compression and Joule–Thomson expansion. Phys. Rev. Lett. **112**, 144504 (2014)
27. Huerta, M.A., Robertson, H.S.: Entropy, information theory, and the approach to equilibrium of coupled harmonic oscillator systems. J. Stat. Phys. **1**(3), 393–414 (1969)
28. Huerta, M.A., Robertson, H.S., Nearing, J.C.: Exact equilibration of harmonically bound oscillator chains. J. Math. Phys. **12**, 2305 (1971)
29. Indeitsev, D.A., Naumov, V.N., Semenov, B.N., Belyaev, A.K.: Thermoelastic waves in a continuum with complex structure. Z. Angew. Math. Mech. **89**, 279 (2009)
30. Inogamov, N.A., Petrov, Y.V., Zhakhovsky, V.V., Khokhlov, V.A., Demaske, B.J., Ashitkov, S.I., Khishchenko, K.V., Migdal, K.P., Agranat, M.B., Anisimov, S.I., Fortov, V.E., Oleynik, I.I.: Two-temperature thermodynamic and kinetic properties of transition metals irradiated by femtosecond lasers. AIP Conf. Proc. **1464**, 593 (2012)
31. Kannan, V., Dhar, A., Lebowitz, J.L.: Nonequilibrium stationary state of a harmonic crystal with alternating masses. Phys. Rev. E **85**, 041118 (2012)
32. Kato, A., Jou, D.: Breaking of equipartition in one-dimensional heat-conducting systems. Phys. Rev. E **64**, 052201 (2001)
33. Khadeeva, L.Z., Dmitriev, S.V., Kivshar, YuS: Discrete breathers in deformed graphene. JETP Lett. **94**, 539 (2011)
34. Klein, G., Prigogine, I.: Sur la mecanique statistique des phenomenes irreversibles III. Physica **19**, 1053 (1953)
35. Kittel, C.: Introduction to Solid State Physics, vol. 8. Wiley, New York (1976)
36. Krivtsov, A.M.: Dynamics of energy characteristics in one-dimensional crystal. In: Proceedings of XXXIV Summer School "Advanced Problems in Mechanics", St.-Petersburg, pp. 261–273 (2007)
37. Krivtsov, A.M.: Energy oscillations in a one-dimensional crystal. Dokl. Phys. **59**(9), 427–430 (2014)
38. Krivtsov, A.M.: Heat transfer in infinite harmonic one dimensional crystals. Dokl. Phys. **60**(9), 407 (2015)
39. Krivtsov, A.M.: The ballistic heat equation for a one-dimensional harmonic crystal. In: Altenbach, H., Belyaev, A., Eremeyev, V.A., Krivtsov, A., Porubov, A.V. (eds.) Dynamical Processes in Generalized Continua and Structures. Springer, Berlin (2019)
40. Krivtsov, A.M., Sokolov, A.A., Müller, W.H., Freidin, A.B.: One-dimensional heat conduction and entropy production. Adv. Struct. Mater. **87**, 197–213 (2018)

41. Kosevich, A.M.: The Crystal Lattice: Phonons, Solitons, Dislocations, Superlattices. Wiley, New York (2006)
42. Kuzkin, V.A., Krivtsov, A.M.: High-frequency thermal processes in harmonic crystals. Dokl. Phys. **62**(2), 85 (2017)
43. Kuzkin, V.A., Krivtsov, A.M.: An analytical description of transient thermal processes in harmonic crystals. Phys. Solid State **59**(5), 1051 (2017)
44. Kuzkin, V.A., Krivtsov, A.M.: Fast and slow thermal processes in harmonic scalar lattices. J. Phys. Condens. Matter **29**, 505401 (2017)
45. Kuzkin, V.A.: arXiv:1808.07255 [cond-mat.stat-mech]
46. Lanford, O.E., Lebowitz, J.L.: Time evolution and ergodic properties of harmonic systems. In: Lecture Notes in Physics, vol. 38, pp. 144–177. Springer, Berlin (1975)
47. Linn, S.L., Robertson, H.S.: Thermal energy transport in harmonic systems. J. Phys. Chem. Sol. **45**(2), 133 (1984)
48. der Linde, D., Sokolowski-Tinten, K., Bialkowski, J.: Laser–solid interaction in the femtosecond time regime. App. Surf. Sci. **109–110**, 1 (1997)
49. Lepri, S., Mejia-Monasterio, C., Politi, A.: A stochastic model of anomalous heat transport: analytical solution of the steady state. J. Phys. A **42**, 2–025001 (2008)
50. Lepri, S., Mejia-Monasterio, C., Politi, A.: Nonequilibrium dynamics of a stochastic model of anomalous heat transport. J. Phys. A: Math. Theor. **43**, 065002 (2010)
51. Marcelli, G., Tenenbaum, A.: Quantumlike short-time behavior of a classical crystal. Phys. Rev. E **68**, 041112 (2003)
52. Mielke, A.: Macroscopic behavior of microscopic oscillations in harmonic lattices via Wigner–Husimi transforms. Arch. Ration. Mech. Anal. **181**, 401 (2006)
53. Mishuris, G.S., Movchan, A.B., Slepyan, L.I.: Localised knife waves in a structured interface. J. Mech. Phys. Solids **57**, 1958 (2009)
54. Murachev, A.S., Krivtsov, A.M., Tsvetkov, D.V.: Thermal echo in a finite one-dimensional harmonic crystal. J. Phys. Condens. Mater. **31**(9), 1 (2019)
55. Prigogine, I., Henin, F.: On the general theory of the approach to equilibrium. I. Interacting normal modes. J. Math. Phys. **1**, 349 (1960)
56. Rieder, Z., Lebowitz, J.L., Lieb, E.: Properties of a harmonic crystal in a stationary nonequilibrium state. J. Math. Phys. **8**, 1073 (1967)
57. Simon, S.H.: The Oxford Solid State Basics. Oxford University Press, Oxford (2013)
58. Schrödinger, E.: Zur dynamik elastisch gekoppelter punktsysteme. Annalen der Physik **44**, 916 (1914)
59. Slepyan, L.I.: On the energy partition in oscillations and waves. Proc. R. Soc. A **471**, 20140838 (2015)
60. Sokolov, A.A., Krivtsov, A.M., Müller, W.H.: Localized heat perturbation in harmonic 1D crystals: solutions for an equation of anomalous heat conduction. Phys. Mesomech. **20**(3), 305–310 (2017)
61. Spohn, H., Lebowitz, J.L.: Stationary non-equilibrium states of infinite harmonic systems. Commun. Math. Phys. **54**, 97 (1977)
62. Tsaplin, V.A., Kuzkin, V.A.: Temperature oscillations in harmonic triangular lattice with random initial velocities. Lett. Mater. **8**(1), 16–20 (2018)
63. Titulaer, U.M.: Ergodic features of harmonic-oscillator systems. III. Asymptotic dynamics of large systems. Physica **70**, 257 (1973)
64. Uribe, F.J., Velasco, R.M., Garcia-Colin, L.S.: Two kinetic temperature description for shock waves. Phys. Rev. E **58**, 3209 (1998)
65. Xiong, D., Zhang, Y., Zhao, H.: Heat transport enhanced by optical phonons in one-dimensional anharmonic lattices with alternating bonds. Phys. Rev. E **88**, 052128 (2013)
66. Ziman, J.M.: Electrons and Phonons. The Theory of Transport Phenomena in Solids, p. 554. Oxford University Press, New York (1960)